IEEE Access
Multidisciplinary | Rapid Review | Open Access Journal

Received April 1, 2019, accepted April 22, 2019, date of publication April 26, 2019, date of current version May 3, 2019.

Digital Object Identifier 10.1109/ACCESS.2019.2913448

Optimal Energy Management of UAV-Based Cellular Networks Powered by Solar Panels and Batteries: Formulation and Solutions

LAVINIA AMOROSI[1], LUCA CHIARAVIGLIO[2,3], (Senior Member, IEEE), AND JAIME GALÁN-JIMÉNEZ[4,5]

[1]DSS Department, Sapienza University of Rome, 00185 Rome, Italy
[2]EE Department, University of Rome Tor Vergata, 00133 Rome, Italy
[3]Consorzio Nazionale Interuniversitario per le Telecomunicazioni, 00133 Rome, Italy
[4]University of Extremadura, 10003 Cáceres, Spain
[5]Instituto de Investigación en Tecnologías Informáticas Aplicadas de Extremadura, 10003 Cáceres, Spain

Corresponding author: Luca Chiaraviglio (luca.chiaraviglio@uniroma2.it)

This work was supported in part by the University of Rome Tor Vergata BRIGHT project (Mission Sustainability Call), in part by the Interreg V-A España-Portugal (POCTEP) 2014-2020 Program (4IE Project (0045-4IE-4P)), in part by the Department of Economy and Infrastructure of the Government of Extremadura under Grant IB16055, Grant IB18030, Grant GR18112, and Grant 2018 Mobility Grants, and in part by the MIUR Project PRIN 2015JJLC3E-PE1.

ABSTRACT We focus on the problem of managing the energy consumption of a cellular network tailored to cover rural and low-income areas. The considered architecture exploits Unmanned Aerial Vehicles (UAVs) to ensure wireless coverage, as well as Solar Panels (SPs) and batteries installed in a set of ground sites, which provides the energy required to recharge the UAVs. We then target the maximization of the energy stored in the UAVs and in the ground sites, by ensuring the coverage of the territory through the scheduling of the UAV missions over space and time. After providing the problem formulation, we face its complexity by proposing a decomposition-based approach and by designing a brand-new genetic algorithm. The results, obtained over a set of representative case studies, reveal that there exists a trade-off between the UAVs battery level, the ground sites battery level, and the level of coverage. In addition, both the decomposed version and the genetic algorithm perform sufficiently close to the integrated model, with a strong improvement in the computation times.

INDEX TERMS Energy management, mixed integer linear programming, renewable energy sources, Unmanned Aerial Vehicles, UAV mission scheduling, cellular networks.

I. INTRODUCTION

Providing cellular connectivity in rural and low-income areas is a complex and challenging task [3]–[5]. This is due to multiple factors, such as the relatively low Return on Investment (RoI) rate for telecom operators, as well as a general lack of electricity derived from the grid. In this context, Base Stations (BSs) mounted on top of Unmanned Aerial Vehicles (UAVs) are a promising solution to bring cellular connectivity [6], [7]. Thanks to the decomposition of the main networking functionalities, in fact, it is possible to install at ground locations most of BS equipment (involving high level tasks, such as baseband processing, handovering functionalities, etc), while keeping on board the UAVs a limited amount of HardWare (HW) providing low level functions (i.e., at signal level). In this way, it is possible to reduce the amount of weight carried by the UAV, and consequently to prolong the duration of the UAV flight. Moreover, another great advantage of such solution is the fact that the UAVs can be used to cover portions of territory, i.e., the ones where the users are located, without the need of covering the whole territory. This allows the operator to notably decrease the costs, compared to a solution in which fixed BSs are used to cover 100% of the territory [8].

Ensuring coverage of a set of areas by means of UAVs is a challenging problem [9]. In fact, the limited amount of battery capacity on board the UAVs imposes to carefully schedule their missions as a sequence of actions over time [1].

The associate editor coordinating the review of this manuscript and approving it for publication was Halil Ersin Soken.

Typical UAV actions include moving from a ground site to an area that needs to be covered, serving the selected areas, returning to the ground site, and recharging the UAV battery on the ground site. This imposes to schedule the UAV missions in a way to preserve as much as possible their battery level.

On the other hand, however, the ground sites at which the UAVs can recharge are also subject to energy constraints [10]. Since in rural and low-income areas the connections to the grid may be not available and/or not reliable [8], the ground sites drain the required energy mainly from micro-generation, by typically exploiting a set of Solar Panels (SPs). In addition, a local battery is used to store the surplus of energy, which can be used during night and/or bad weather conditions. Clearly, also this system needs to be carefully managed, in order to ensure the recharging of the UAVs that have depleted their battery.

In this context, several questions emerge, such as: Is it possible to define a framework to cover a set of areas by means of the UAVs and manage their energy consumption? How to leverage the trade-off between the energy stored in the ground sites (for future needs) and the energy stored in the UAVs (used to perform their missions)? Is it possible to define efficient strategies to solve this problem in a reasonable amount of time? The goal of this work is to shed light on these issues. More in depth, we initially provide a complete problem formulation which is able to: i) balance the energy stored in the ground sites and the battery level of the UAVs, ii) schedule the UAVs missions as a sequence of actions over time, iii) ensure coverage of a set of areas. We then face the complexity of the problem, by introducing a decomposed version as well as by designing a sub-optimal heuristic, which are able to notably decrease the amount of time to retrieve a solution. In addition, we introduce a parameter to weigh differently the battery level of the UAVs w.r.t. the energy stored in the ground sites, thus allowing the operator to carefully leverage the trade-off between these two terms, by properly varying the weight of each term in the objective function. Our results, obtained over different case studies, demonstrate that it is possible to cover the set of areas by means of the UAVs, while controlling the amount of energy stored in the ground sites and the UAVs battery level. In addition, we also show that both the decomposed version and the proposed heuristic are sufficiently close to the integrated problem.

To the best of our knowledge, none of the previous work has conducted a similar analysis. Actually, the closest papers to our work are [1], [2], in which the authors target the minimization of the energy due to the moving actions for a set of UAVs, by providing the problem formulation and a simple heuristic, which is based on a genetic algorithm. Compared to them, in this work we go five steps further by: i) targeting a different problem, which includes the maximization of the energy stored by the UAVs and the one stored in the batteries of the ground sites, ii) introducing a model decomposition to solve the problem also for large instances, iii) defining a new heuristic approach tailored to the considered problem, iv) solving the problem in different scenarios, ranging from a small one to a large-scale case study, which is composed of dozens of ground sites and hundreds of areas to be covered, v) thoroughly comparing the solutions obtained from the integrated problem, the decomposed one, and the proposed heuristic.

The remainder of the paper is organized as follows. Sec. II reviews the related work. Sec. III describes the considered UAV-based cellular architecture. The problem formulation is reported in Sec. IV. The proposed decomposition approach is detailed in Sec. V. Sec. VI describes the proposed genetic algorithm. Sec. VII thoroughly describes the scenarios and the setting of the input parameters. Sec. VIII reports the performance evaluation of the proposed solutions. Sec. IX reports a discussions of the main issues impacting our approach. Finally, Sec. X concludes our work.

II. RELATED WORK

We divide the related work in three categories: i) optimization for UAVs usage in civil applications, ii) UAV-based networks, and iii) UAVs mission planning.

A. OPTIMIZATION FOR UAVS USAGE IN CIVIL APPLICATIONS

In the recent years, the number of fields where UAVs are commonly used to improve people's quality of life has significantly increased, thanks to the easy-going features and acceptable costs of such solution. A great variety of civil applications currently use UAVs to improve their operation and to save the costs, e.g., high-precision surveillance, package delivery or disasters management. To this aim, we refer the interested reader to the work of Otto *et al.* [11], who provide a comprehensive survey of optimization approaches for civil applications using UAVs. Hayat *et al.*, in turn, report in [12] the characteristics and requirements of UAV-based networks for envisioned civil applications from a communications and networking point of view.

One of the most common applications where UAVs are being widely used is video surveillance [13]. Trotta *et al.* [14] target the design of a multi-hop wireless network composed of UAVs to perform city-scale video monitoring, while considering energy consumption constraints. More in depth, a set of Points of Interest (PoIs) are covered by the UAV-based network. Their solution includes public transportation buses to: i) allow the UAVs recharge their batteries on top of them, and ii) carry the UAVs to the next PoI to record. In contrast to them, in this work we focus on a different scenario, where the UAVs are used to deploy a cellular network, with the goal of providing coverage to the users located inside a particular set of areas.

Motlagh *et al.* [15] propose a UAV-based Internet of Things (IoT) platform for crowd surveillance where face recognition is applied to identify suspicious individuals. Since UAVs have a limited processing power, video processing is offloaded to mobile edge computing nodes, with the

aim of extending their batteries for surveillance purposes. Clearly, when the recording of the people is performed, visual privacy has to be strictly taken into account, as also reported by Clarke [16]. Similarly to these works, in this paper we also face the energy limitation of UAVs batteries. However, our work is tailored to the cellular service, and not video surveillance like in [15], [16]. Moreover, another original aspect of our work is that we exploit the SPs and batteries installed on specific ground sites to allow UAVs recharge when necessary. In addition, we jointly target the maximization of UAVs battery level and the maximization of the sites battery levels in a multi-objective function.

Another type of application in which UAVs are widely exploited is the so-called delivery-by-drone logistics system. In this context, the main idea is to use autonomous UAVs for small parcel delivery. Specifically, each UAV holds a container where the parcel is loaded and moves it from the distribution center (warehouse) to the destination customer. The parcel is then dropped off near the customer's front door and the UAV returns to the starting point without human interaction (see e.g., the work of Gross [17]). Research efforts have been made on this particular application, mainly focused on the technical aspects of UAVs such as endurance/safety of UAVs and the selection of the distribution centers in order to be as much efficient as possible. Specifically, Song *et al.* [18] propose a Mixed Integer Linear Programming (MILP) formulation and an efficient heuristic for derivation of persistent UAV delivery schedules. In their work, UAVs can share multiple distribution centers across the field of operation to reload products and recharge their batteries. With this approach, the flight-time and loadable-product limitations of UAVs can be overcome, whilst a persistent delivery service can be achieved. Moreover, Murray and Chu [19] exploit the combination of traditional truck delivery with the use of autonomous UAVs that can be launched from the truck, especially for cases where the distribution center is far away from customers. Although with this method the coverage range to deliver parcels is significantly increased, a human interaction (i.e., the driver) is required to load parcels into the UAVs and replace batteries during long trips. This idea is also exploited by Poikonen *et al.* [20], where the goal is to minimize the completion time to deliver all the packages and to return all the trucks back to the central depot.

Although these works prove that there is a great interest in exploiting the UAVs for persistent package delivery while covering a wide area, the goal of this work is to provide a different service, i.e., the wireless coverage to users by means of UAV-based BSs, which are able to fly and complete their missions without requiring any human interaction.

B. UAV-BASED NETWORKS

Recently, the optimal planning and management of networks composed by UAVs has gained attention from the research community. Drone networking is a recent research topic where UAVs are intended to serve as a basic element to sense and relay information in the next generation of wireless networks. In [21], Bor-Yaliniz *et al.* introduced the UAV-BS concept, in which a BS is mounted on top of a UAV in order to complement terrestrial heterogeneous networks (HetNets). A multi-tier drone-cell network is proposed to bring the supply of wireless networks exactly to the place and time where the demand is required. Mozaffari *et al.* analyze in [22] the performance of a UAV-BS in which users can also communicate via direct device-to-device links. In particular, their main goal is to maximize the coverage provided by a UAV to a particular area by considering two types of communications: i) downlink UAV-to-user communication, and ii) underlaid device-to-device communication, which can generate potential interferences and affect i). In a recent work, Bor-Yaliniz *et al.* [23] open a discussion about the set of challenges that arise when combining the concept of UAVs and wireless networks from the 5G perspective in order to support network performance.

One of the most promising field of UAV-based networks is natural disaster management, where UAVs can be combined with Wireless Sensor Networks (WSN) in order to find injured people and report their location to rescue teams. To this aim, Adams and Friedland [24] review the related works in which UAVs are used for imagery collection during the phase of disaster monitoring. Maza *et al.* [25] exploit the coordination of multiple UAVs to propose a distributed decision-making architecture for challenging scenarios, such as disaster management or civil security applications. The smooth integration of autonomous vehicles from different vendors and the low communication cost derived from the distributed scheme make this approach particularly appealing. In contrast to them, the problem of this work is devoted to the scheduling of the UAVs missions by taking into account the coverage of the areas, as well as the constraints on UAVs battery level and on the battery level of ground sites.

Asadpour *et al.* [26] propose an ad-hoc multi-hop UAV networking solution, which is able to: i) establish end-to-end connectivity to the smartphone of a missing person, and ii) stream high-resolution videos for scanning areas and spotting injured and missing people. One step further, Malandrino *et al.* [27] exploit the use of UAVs to improve wireless network coverage during a disaster crisis by complementing or replacing the traditional -yet affected- communication infrastructure. An optimization problem is presented to provide the best possible coverage while maximizing user throughput. A similar approach is followed by the seminal work of Erdelj and Natalizio in [28], where a wireless communication network exploiting UAVs is created between survivors, rescue teams and still operating cellular infrastructure. Erdelj *et al.* [29] also survey the related works on the joint role of WSN and UAVs for natural disaster management and present a set of unsolved challenges whose solution would significantly improve the efficiency of disaster management systems. One step further, Erdelj *et al.* [30] classify different types of disasters considering geophysical, climate-induced and meteorological issues, and propose suitable WSN and UAV-based network architectures for

each category. Eventually, an IoT-UAV ecosystem is devised by Erdelj *et al.* [31], in order to provide real-time data and multimedia communications in unstable communication environments by means of a multi-UAV system, which also offers on-demand usage of available sensors, smartphones and UAV infrastructure.

Quality-of-Experience (QoE) of mobile users can also be improved by means of UAV-based networks. Chen *et al.* [32] propose to use cache-enabled UAVs to provide the required QoE to mobile users within a Cloud Radio Access Network (C-RAN) by minimizing the UAVs transmit power and reducing the transmission delay in the system. By exploiting machine learning techniques, human-centric information is used to predict both content distribution and users' mobility patterns. Such learned information is then used to determine UAVs placement and the content to cache. One step further, gathered information from users can be of great value also to enhance, e.g., the energy efficiency of wireless networks [33].

In [34], Yanmaz *et al.* summarize the existing challenges for the design of a system with multiple small UAVs. A high-level architecture composed of UAVs and ground stations with sensing, coordination and communication features is proposed and evaluated in several real-world applications with different demands and constraints, such as the assistance during a disaster, documenting the progress of a large construction site, and the process of search and rescue. As conclusion, the authors remark that an effective design of UAVs network is given by the proper definition of the interactions between sensing, coordination, and communication modules, as well as with the specific constraints imposed by the application.

The work of Sánchez-García *et al.* [35] combines the common features of aerial and aquatic wireless ad hoc networks to apply existing solutions that are valid for the aerial medium to the aquatic one. The authors also survey evaluation tools for this kind of scenarios and provide a set of open challenges about the design and evaluation of both types of networks. Reina *et al.* [36] target the selection of the UAVs positions in the 2D-space in order to ensure a connected network with redundancy and fault tolerant constraints. Our goal is instead to schedule the UAV missions by considering the possible UAV actions/movement which are passed to our problem as the arcs in a multi-period graph. Actually, the output of [36] can be used as input to our problem.

Although these works prove that there is a great interest in exploiting UAVs for communications and monitoring, in this work we focus on a different aspect, i.e., the provisioning of cellular service in rural and low-income areas by exploiting UAVs carrying BSs and powered solely by renewable energy sources. Moreover, we target the efficient management of the battery levels both at the ground sites and at the UAVs.

C. UAVS MISSION PLANNING

We finally review the works focused on the problem of UAVs mission planning. As in the case of previous categories, different applications require the planning of the missions of a set of UAVs.

In the context of the coverage of sports events, Zema *et al.* [37] introduce the sport event filming problem with communication and connectivity constraints, where a court or sport field is covered by a coordinated fleet of UAVs and the spectators receive on their personal devices a high-quality video live stream of the game. The target objective function is the maximization of viewers' satisfaction as well as the minimization of the distance traveled by the UAVs. Simulations over representative case-studies show that the performance of the proposed scheme outperforms other related works in terms of packet loss and achieved coverage. In contrast to them, the main differences with our work are twofold: i) each area is served by a single UAV, and ii) we maximize both UAVs battery level and the available battery level on sites while respecting coverage and power consumption constraints.

The vehicle routing problem for UAV delivery is studied by Dorling *et al.* [38]. Karaman and Frazzoli [39] further generalize this problem by introducing a MILP formulation that integrates complex tasks and constraints in UAVs missions. This problem is further analyzed by Lamont *et al.* [40], where a multi-objective evolutionary algorithm is presented to tackle the 3D vehicle routing with the use of UAV swarms.

However, UAVs mobility is highly dependent on the specific missions they have to perform. Changes in a UAV-based network topology due to the pre-defined movements of the swarm of UAVs can negatively affect to the network performance. In this way, the topology management problem is deeply studied also in the scope of this type of dynamic scenarios in order to ensure an acceptable network performance. In [41], Kim *et al.* propose a solution to create a UAV-based network topology from the scratch, by adapting it to the topological changes caused by the unpredictable mission-based movements of UAVs. To do that, they rely on the presence of special nodes, namely Relaying UAVs (RUs), to relay data between adjacent UAVs, with the aim of supporting reliable communications in the UAV-ground site wireless link and maximizing the network performance. Differently from other works, the dependency between such metric and the routing protocol is considered in the proposed Particle Swarm Optimization (PSO) metaheuristic. Magán-Carrión *et al.* [42] also use PSO to solve the topology problem in generic Mobile Ad-Hoc Network (MANET) scenarios. A centralized multi-stage methodology is applied, in which the deployment and movement of relaying nodes contribute to maximize both network connectivity and throughput.

The limited battery of UAVs has also opened a niche for the research community to propose solutions with the aim of extending the duration of UAV missions. The robustness aspects of the problem are studied by Evers *et al.* [43], where the uncertainty in the fuel usage between targets (e.g., due to weather conditions) is considered. Eventually, Kim *et al.* [44] propose a system in which multiple-shared bases located in different geographical places are used by UAVs to recharge

their batteries, therefore supporting long term duration missions. In particular, their goal is to minimize the total travel distance of the UAVs fleet taking into account power consumption and recharging constraints. This problems differs, e.g., from the one studied by Trotta *et al.* [9], where the focus is to maximize geographical coverage by exploiting the 3D placement problem in conjunction with the scheduling of the UAVs recharging actions at ground sites. In contrast to these works, we aim at maximizing the combination of the battery level of UAVs and the one at ground sites for all day wireless coverage provisioning.

Amorosi *et al.* [1] propose an optimization framework to schedule UAVs missions, with the goal of providing cellular coverage in rural areas while minimizing the energy consumed by UAVs when moving from the ground sites to a set of areas. In addition, a set of SPs is considered to recharge UAVs batteries. Eventually, the considered MILP formulation exploits a graph-based structure to optimally model the UAVs missions by solving a variant of an unsplittable multi-commodity flow problem defined on a multi-period graph. Since the aforementioned problem is known to be NP-hard (see, e.g., the work of D'Andreagiovanni *et al.* [45]), a simple heuristic to practically solve it is proposed by Galán-Jiménez *et al.* [2]. In contrast to them, in this work we consider a different problem, where the main goal is to target the maximization of the battery levels of the ground sites and of the UAVs, while ensuring cellular coverage. In addition, we target the solution of the problem over large scenarios. These issues are tackled in this work by: i) designing new approaches based on decomposition methods and genetic algorithms to practically solve the optimization problem, ii) introducing a multi-objective function, in order to properly balance both the UAVs and the ground sites battery levels.

III. ARCHITECTURE DESCRIPTION

We briefly describe the considered UAV-based cellular architecture, whose main functionalities are implemented as 5G components. We refer the reader to [5], [8] for a comprehensive description. In brief, we assume that most of BS equipment, and in particular the dedicated HW one, is carried on board of the UAV. The dedicated HW includes a Remote Radio Head (RRH) and part of the Base Band Unit (BBU), which ensure low-level tasks on the communication between the UAV-based BS and the user equipment. The RRH is connected to a set of antennas that are also carried by the UAV. The remaining tasks (which are performed by higher layers) are realized by virtualized elements installed on the commodity HW, which is placed at a ground site. The separation between high-level and low-level functionalities is peculiar of next-generation cellular equipment, like the forthcoming 5G. This solution reduces the amount of HW carried by the UAV, and consequently tends to prolong the duration of the flight compared to the case in which all the functionalities are carried on the UAV (thus increasing its weight). Finally, the high-level HW functionalities hosted at the ground site and the low-level ones carried on board of the UAV need to establish a radio link (separated from the ones between the UAV and the users), which has to guarantee high levels of reliability.

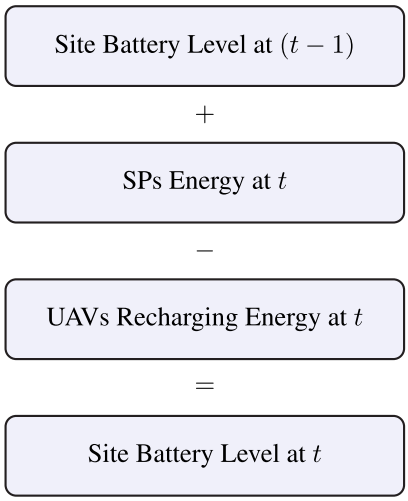

FIGURE 1. Ground site battery level balance.

The considered architecture can be extended also to pre-5G networks, like 4G. However, bringing the 4G radio functionalities on board the UAV is more challenging than in a 5G scenario, due to the fact that 4G Base Stations (BSs) are pretty monolithic and less flexible compared to 5G ones. For example, a 4G BS would likely require to bring on board the UAV a large amount of HardWare (HW), due to the fact both low level functionalities and high level ones are typically run on the same set of devices. On the other hand, bringing 5G equipment seems a more viable solution, due to the fact that the 5G BS functionalities can be split over a set of devices, part of them located at ground and other ones placed on the UAV. This architecture allows to decrease the weight of the UAV, and thus increasing the duration of the UAV flight.

Apart from hosting the commodity HW, each site is connected to a set of SPs and batteries, which are installed in the same site location. In particular, we assume that SPs and batteries are the only sources of energy (i.e., no connection is requested to the grid). On the other hand, the UAVs are equipped with batteries, and they are recharged by a ground site when needed. We also assume that the total amount of time is discretized in a set of Time Slots (TSs). In each TS, the battery level of the ground site is computed as the composition of different terms, as reported in Fig. 1. In particular, an amount of energy may be derived from SPs (if the energy from the sun is available). Moreover, an amount of energy may be used to recharge the UAVs that have depleted their batteries. At last, the remaining energy is stored in the battery for the following TSs. Clearly, the battery level is kept between a minimum and a maximum value. Without loss of generality, we assume that, in case there exists a surplus of energy coming from SPs, which is not used by UAVs that are being recharged and which is higher than the maximum battery level, the battery level is saturated to the

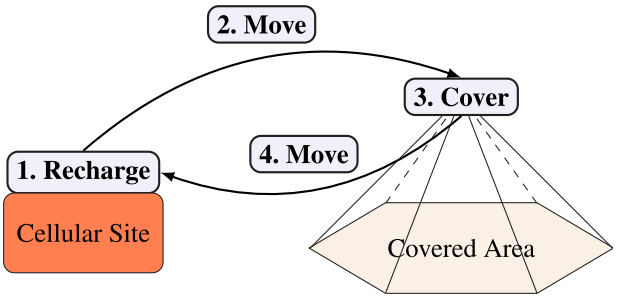

FIGURE 2. A typical UAV mission requiring recharging, moving and covering actions.

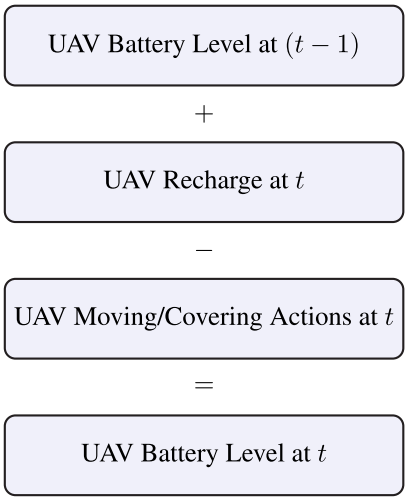

FIGURE 3. UAV battery level balance.

maximum one. In addition, we always ensure a minimum battery level. In particular, this constraint is critical to prevent battery failures, which may occur when the battery is completely depleted [10].

We then detail the main UAVs features assumed in this work. Fig. 2 shows an example of a typical mission performed by a UAV carrying a BS. In particular, each UAV has a battery of a given (limited) capacity. The battery may be initially recharged by draining an amount of energy from the ground site. In the following, the UAV moves from the ground site to the area to be covered. When the area to be covered is reached, the UAV activates the BS functionalities In the following, the UAV moves back to the ground site. Similarly to the ground sites, the UAV needs to ensure a battery level balance, which is reported in Fig. 3. In addition, the battery level is always kept between a minimum level and a maximum one.

IV. PROBLEM FORMULATION

We model the problem as a Mixed Integer Linear Programming (MILP), tracing it back to a variant of the unsplittable multicommodity flow problem defined on a multiperiod graph. More formally, we denote: i) by $\mathcal{A}$ the set of areas to be covered; ii) by $\mathcal{S}$ the set of available ground sites; iii) by $\mathcal{D}$

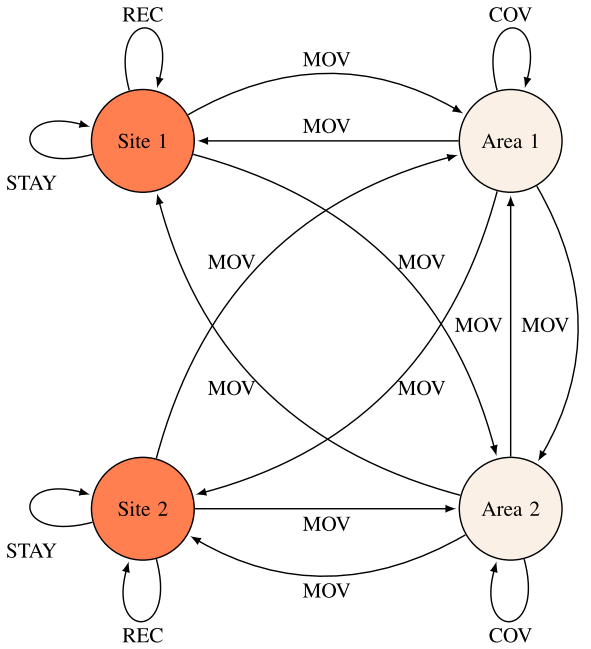

FIGURE 4. Set of UAV actions between two sites and two areas to be covered. Each action is represented as an arc between two places and consumes one TS.

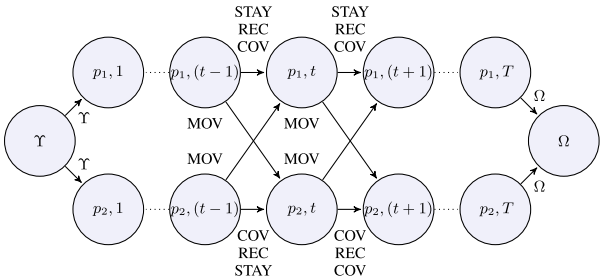

FIGURE 5. General arc transitions between consecutive TSs. The source node Υ, a set of two places $\{p_1, p_2\}$, and the final sink node Ω are shown.

the set of UAVs; iv) by $\mathcal{T} = \{0, 1, 2, \ldots, |\mathcal{T}|\}$ the set of Time Slots (TSs). We also define the set of places $\mathcal{P}$, obtained as the union of the set of areas and sites (i.e., $\mathcal{P} = \mathcal{A} \cup \mathcal{S}$). In each TS each UAV can perform one among the following actions:

- REC: the UAV recharges itself at a given site;
- STAY: the UAV is idle at a given site (not consuming any energy);
- MOV: the UAV moves from a site to an area, or from an area to another area, or from an area to a site;
- COV: the UAV covers a given area.

Each of the aforementioned actions requires one TS to be executed. An example of possible actions performed by the UAVs between two sites and two areas is reported in Fig. 4.

In order to model the actions performed by the UAVs over the considered set of TSs, a multiperiod directed graph $G(\mathcal{N}, \mathcal{L})$ is introduced. The set of nodes $\mathcal{N}$ includes one node (p, t) for each place $p \in \mathcal{P}$ and for each TS $t \in \mathcal{T}$. In addition, we add to the set of nodes one source node Υ and one sink node Ω to track the UAVs paths. We denote a generic

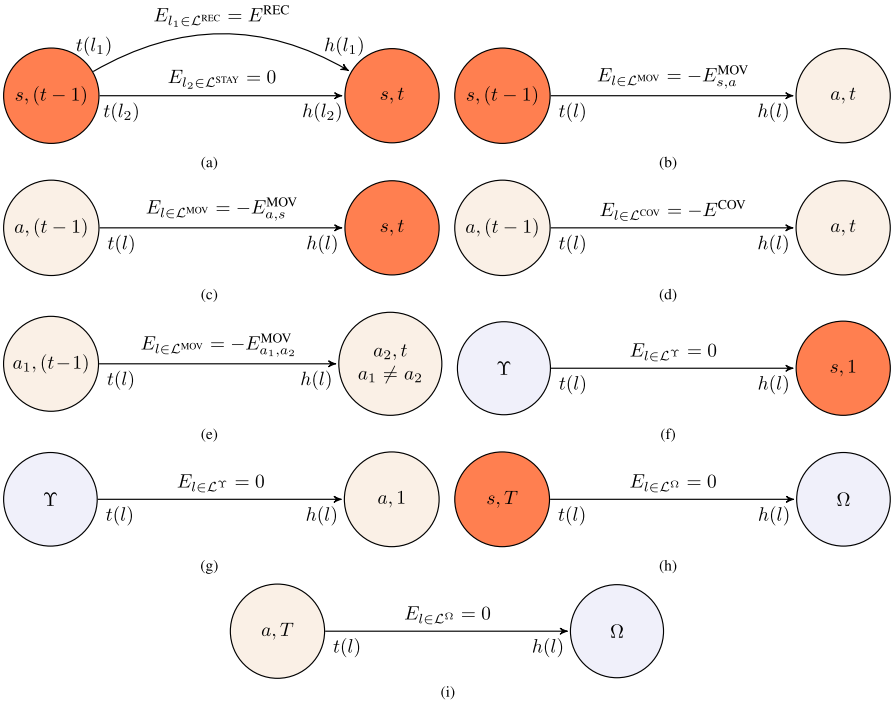

FIGURE 6. Admissible arcs and energy values for each pair of places and consecutive TSs.

arc $l \in \mathcal{L}$ by $[(p_1, t_1), (p_2, t_2)]$, where $t(l) = (p_1, t_1)$ and $h(l) = (p_2, t_2)$ are the tail and the head of the arc, respectively. We then introduce the set of arcs $\mathcal{L}^{\text{REC}}$, $\mathcal{L}^{\text{STAY}}$, $\mathcal{L}^{\text{MOV}}$ and $\mathcal{L}^{\text{COV}}$ to denote the admissible transitions between (p_1, t_1) and (p_2, t_2) for the recharging, staying, moving and coverage actions, respectively. Additionally, we define the sets $\mathcal{L}^{\Omega}$ and $\mathcal{L}^{\Upsilon}$ connecting the source node to all places at the first TS and all places at the last TS to the sink node, respectively. The union of sets $\mathcal{L}^{\text{REC}} \cup \mathcal{L}^{\text{STAY}} \cup \mathcal{L}^{\text{MOV}} \cup \mathcal{L}^{\text{COV}} \cup \mathcal{L}^{\Upsilon} \cup \mathcal{L}^{\Omega}$ defines the entire set of links $\mathcal{L}$. Fig. 5 shows the admissible arcs for a toy case example composed of two places. To ease the figure, we collapse in a single arc all the parallel links between two nodes in the graph.

In the following, we associate an energy weight for each arc in $\mathcal{L}$, as reported in Fig. 6. More in detail, when the UAV does not change the site between two consecutive TSs, STAY and REC links are defined (Fig. 6(a)). Specifically, when the UAV is recharging the link weight is E^{REC}. Alternatively, when the UAV is in the STAY state, the link weight is zero (i.e., the UAV does not consume any energy). In addition, when the UAV moves from a site $s \in \mathcal{S}$ to an area $a \in \mathcal{A}$ (Fig. 6(b)), an arc $l \in \mathcal{L}^{\text{MOV}}$ is defined.[1] In this case, the link weight is $-E^{\text{MOV}}_{s,a}$, which denotes the amount of energy consumed for moving the UAV from site s to area a. Similarly, when the UAV moves from an area a to a site s (Fig. 6(c)), a link $l \in \mathcal{L}^{\text{MOV}}$ is introduced, with weight equal to $-E^{\text{MOV}}_{a,s}$. On the other hand, when the area is not changed (Fig. 6(d)), the UAV performs a coverage action. In this case, the corresponding link $l \in \mathcal{L}^{\text{COV}}$ has a weight of $-E^{\text{COV}}$, denoting the amount of energy spent to cover an area in one TS. Eventually, when the UAV moves from area $a_1 \in \mathcal{A}$ to a different area $a_2 \in \mathcal{A}$ (Fig. 6(e)), a link $l \in \mathcal{L}^{\text{MOV}}$ with weight $-E^{\text{MOV}}_{a_1,a_2}$ is introduced. Finally, the links connecting Υ and Ω to the other nodes are defined in Fig. 6(f)-6(i). Clearly, such links do not consume any amount of energy, since both Υ and Ω are fictitious nodes. Consequently, their energy weight is set to zero.

We then introduce the following decision variables:

1) binary flow variable $f^d_l \in \{0, 1\}$ $\forall\, l \in \mathcal{L}, d \in \mathcal{D}$, equal to 1 if the UAV d uses the arc l (0 otherwise);
2) binary variable $z^t_a \in \{0, 1\}$ $\forall\, a \in \mathcal{A}, t \in \mathcal{T}$ equal to 1 if area a is not covered in TS t (0 otherwise);
3) continuous variable $b^t_s \geq 0$ $\forall\, s \in \mathcal{S}, t \in \mathcal{T}$, representing the battery level of site s at TS t;
4) continuous variable $e^t_d \geq 0$ $\forall\, d \in \mathcal{D}, t \in \mathcal{T}$, representing the battery level of UAV d at TS t.

The overall Optimal Energy Management of UAV-based cellular networks (EMUC) problem is then formulated as:

$$\max\Big(\sum_{s\in\mathcal{S}}\sum_{t\in\mathcal{T}} b^t_s + \alpha \cdot \sum_{d\in\mathcal{D}}\sum_{t\in\mathcal{T}} e^t_d - \gamma \cdot \sum_{a\in\mathcal{A}}\sum_{t\in\mathcal{T}} z^t_a\Big) \tag{1}$$

$$\text{Subject to: } \sum_{\substack{l\in\mathcal{L}:\\ h(l)=(p,t)}} f^d_l - \sum_{\substack{l\in\mathcal{L}:\\ t(l)=(p,t)}} f^d_l = \beta^d_{(p,t)}$$
$$\forall p \in \mathcal{P}, d \in \mathcal{D}, t \in \mathcal{T} \tag{2}$$

[1] The set $\mathcal{L}^{\text{MOV}}$ may not include all the possible links between each pair of places. This occurs, e.g., when a maximum distance between a UAV and the ground site has to be ensured.

$$\sum_{d\in\mathcal{D}}\sum_{\substack{l\in\mathcal{L}^{\mathrm{COV}}:\\ h(l)=(a,t)}} f_l^d + z_a^t = 1,\ \forall a\in\mathcal{A}, t\in\mathcal{T} : t\geq 1 \tag{3}$$

$$b_s^t \leq b_s^{t-1} + E_s^t \cdot N_s^{\mathrm{SP}} - \sum_{d\in\mathcal{D}} E_l \cdot f_l^d,\ \forall s\in\mathcal{S}, t\in\mathcal{T},$$

$$\forall l \in \mathcal{L}^{\mathrm{REC}} : h(l) = (s,t) \wedge t(l) = (s,t-1) \tag{4}$$

$$B^{\mathrm{MIN}} \cdot N_s^{\mathrm{B}} \leq b_s^t \leq B^{\mathrm{MAX}} \cdot N_s^{\mathrm{B}},\quad \forall s\in\mathcal{S}, t\in\mathcal{T} \tag{5}$$

$$e_d^t \leq e_d^{t-1} + \sum_{\substack{l\in\mathcal{L}^{\mathrm{MOV}}\cup\mathcal{L}^{\mathrm{REC}}\cup\mathcal{L}^{\mathrm{COV}}:\\ t(l)=(*,t-1)\\ h(l)=(*,t)}} E_l \cdot f_l^d$$

$$\forall d\in\mathcal{D}, t\in\mathcal{T} \tag{6}$$

$$E^{\mathrm{MIN}} \leq e_d^t \leq E^{\mathrm{MAX}},\quad \forall d\in\mathcal{D}, t\in\mathcal{T} \tag{7}$$

Under variables: $f_l^d \in \{0,1\}\ \forall\, l \in \mathcal{L}, d \in \mathcal{D}$, $z_a^t \in \{0,1\}\ \forall\, a \in \mathcal{A}, t \in \mathcal{T}$, $b_s^t \geq 0\ \forall\, s \in \mathcal{S}, t \in \mathcal{T}$, $e_d^t \geq 0\ \forall\, d \in \mathcal{D}, t \in \mathcal{T}$.

The objective function (1) is the maximization of the site battery level and the UAV one. A parameter α is used to change the weight of the UAV battery level w.r.t. to the one of the ground sites. When $\alpha << 1$ the problem tends to maximize the ground site battery level, thus possibly limiting the amount of energy stored by the UAVs. This policy is useful to preserve the ground sites battery level when, e.g., the energy from SPs is not available. On the other hand, when $\alpha >> 1$ the EMUC problem tends to pursue the maximization of the energy stored by the UAVs, thus (possibly) involving frequent recharging actions at the ground sites. This policy is effective when it is critical to preserve the UAV battery level, e.g., to always ensure that each UAV has enough battery to complete a mission. Finally, the last term of (1) is a penalty associated when an area is not covered by a UAV. In this case, in fact, there is a loss of connectivity. We model this aspect by multiplying the Boolean variables z_a^t for a penalty weight γ. Note that, for sufficiently large values of γ, an area may be not covered due to two main reasons: i) no UAV can serve the area, ii) the current instance of the problem cannot guarantee full coverage of the whole set of areas. The first aspect can be overcome by imposing a sufficiently large set of UAVs (as done in this work). The second issue instead may arise from the problem decomposition, which is described in the following section.

Focusing then on constraints (2)-(7), (2) impose the conservation of the flow variables f_l^d, where the term $\beta^d(p,t)$ appearing in the constraint is defined in Tab. 1. The coverage of each area is imposed through constraints (3), by considering only the $\mathcal{L}^{\mathrm{COV}}$ arcs incoming to each area. This constraint also sets the variable z_a^t when it is not possible to cover area a at TS t. Constraints (4) impose then the battery balance for each TS t and for each site s. The balance is computed by adding to the battery level at previous TS the energy produced by the SPs (equal to the production of energy of a single SP E_s^t times the total number of installed SPs N_s^{SP}) minus the energy requested to recharge the UAVs at current TS. In addition, the minimum and the maximum battery levels are enforced by constraints (5), where N_s^{B} is the total number of batteries installed in site s. In the following, we set the UAV battery level through constraints (6), by considering: i) the contributions of the $\mathcal{L}^{\mathrm{MOV}}\cup\mathcal{L}^{\mathrm{REC}}\cup\mathcal{L}^{\mathrm{COV}}$ energy arcs used by the UAV at the current TS, ii) the UAV energy at previous TS. The minimum and the maximum UAV battery levels are then ensured by constraints (7).

TABLE 1. Setting of the $\beta^d(p,t)$.

Condition	$\beta^d(p,t)$ Value
$(p,t) = \Omega$	1
$(p,t) = \Upsilon$	-1
otherwise	0

We then focus in more detail on constraints (4)-(7), and in particular on the reason why an inequality is set in constraints (4) and (6) instead of equality. Actually, both the battery and the energy levels have to be lower than the maximum values appearing in (5) and (7), namely $B^{MAX} \cdot N_s^{\mathrm{B}}$ and E^{MAX}. When solving the model, the values of the variable b_s^t and variable e_d^t will be the minimum between the expression in (4) and $B^{MAX} \cdot N_s^{\mathrm{B}}$ and between the expression in (6) and E^{MAX}, respectively. However, as we maximize both battery and energy levels, constraints (4) and (6) will be active in all cases in which the right hand side of (4) and (6) is less than or equal to $B^{MAX} \cdot N_s^{\mathrm{B}}$ and E^{MAX}, respectively.

V. PROBLEM DECOMPOSITION

The EMUC problem is challenging to be solved, due to the fact that the underlying multi-period graph tends to grow very quickly as the total number of places and the total number of TSs are increased. To tackle this issue, we apply a *divide et impera* approach, which is based on the decomposition of the original problem in subproblems of smaller size, each of them (potentially) easier to be solved compared to EMUC. More in depth, we split the original problem into sub-problems by first introducing a spatial decomposition between the ground sites, and then by including a temporal decomposition across the set of TSs. In the following, we detail the two decomposition approaches, and then we sketch the entire methodology.

A. SPATIAL DECOMPOSITION

We initially split the original problem into a set of subproblems, each of them including a single ground site. For each ground site $s \in \mathcal{S}$, we find a set partition of $\mathcal{A}$ by identifying a cluster $\mathcal{A}_s$ of areas that will be covered only by UAVs whose missions originate/terminate solely from/in s. This partition is found according to a minimum cost rule, which is expressed as the amount of energy consumed by a UAV for moving from a given ground site to a given area. More formally,

the following optimization problem is solved:

$$\min \sum_{l \in \mathcal{L}^{\mathrm{MOV}}: t(l) \in \mathcal{S}, h(l) \in \mathcal{A}} E_l \cdot x_l \tag{8}$$

Subject to:

$$\sum_{l \in \mathcal{L}^{\mathrm{MOV}}: t(l) \in \mathcal{S}, h(l) = a} x_l = 1, \quad \forall a \in \mathcal{A} \tag{9}$$

$$x_l \in \{0, 1\}, \quad \forall l \in \mathcal{L}^{\mathrm{MOV}} : t(l) \in \mathcal{S}, h(l) \in \mathcal{A} \tag{10}$$

where the binary variable $x_l \in \{0, 1\}$ $\forall l \in \mathcal{L}^{\mathrm{MOV}}$ is equal to 1 if area $h(l) \in \mathcal{A}$ is assigned to the ground site $t(l) \in \mathcal{S}$ and 0 otherwise. The solution of this set partitioning model provides the clusters of areas associated with the ground sites and reduces the problem size. However, due to the temporal dimension of the problem, the size of the multi-period graph underlying the model remains quite large and its resolution to optimality is still challenging. Thus, we introduce an additional level of decomposition, which is detailed in the following subsection.

B. TEMPORAL DECOMPOSITION

In order to further reduce the size of each problem instance, we apply a temporal decomposition on each cluster A_s. Specifically, we split the set of TSs $\mathcal{T}$ into subsets of consecutive TSs, denoted as $\mathcal{T}_i$ (each of them with the same cardinality), such that $\mathcal{T} = \mathcal{T}_1 \cup \mathcal{T}_2 \cup ... \mathcal{T}_n$. Clearly, in order to ensure the continuity of the UAV missions as well as the proper computation of the battery levels of the ground sites and of the UAVs, we need to include an additional set of constraints. More in depth, the UAVs location at the first TS of subset $\mathcal{T}_i$ must be equal to the one of the last TS of the previous subset $\mathcal{T}_{i-1}$, as guaranteed by the following constraint:

$$\sum_{\substack{l \in \mathcal{L}: \\ t(l) = (p, T_i(1))}} f_l^d = 1, \quad \forall d \in \mathcal{D}, \forall p \in \mathcal{A}_s : I(d) = p \tag{11}$$

where $T_i(1)$ is the first TS of the subset $\mathcal{T}_i$ and $I(d)$ $\forall d \in \mathcal{D}$ represents the position of the UAV d at the last TS of the previous subset $\mathcal{T}_{i-1}$. In addition, the UAVs battery level at the first TS of subset $\mathcal{T}_i$ must be equal to the one of the last TS of the previous subset $\mathcal{T}_{i-1}$, denoted by E_d^{IN} $\forall d \in \mathcal{D}$, as imposed by the following constraint:

$$e_d^{T_i(1)} = E_d^{\mathrm{IN}}, \quad \forall d \in \mathcal{D} \tag{12}$$

Moreover, the battery level of the ground site at the first TS of subset $\mathcal{T}_i$ must be equal to the one of the last TS of the previous subset $\mathcal{T}_{i-1}$:

$$b^{T_i(1)} = B^{\mathrm{IN}} \tag{13}$$

where B^{IN} is the battery level of the recharging site at the last TS of the previous subset $\mathcal{T}_{i-1}$.

The variables for each subset $\mathcal{T}_i$ are then retrieved by solving the following problem:

$$\max\Big(\sum_{s \in \mathcal{S}} \sum_{t \in \mathcal{T}_i} b_s^t + \alpha \cdot \sum_{d \in \mathcal{D}} \sum_{t \in \mathcal{T}_i} e_d^t - \gamma \cdot \sum_{p \in \mathcal{A}} \sum_{t \in \mathcal{T}_i} z_a^t\Big) \tag{14}$$

subject to (2)-(7),(11)-(13), by considering only the subset of areas in cluster $\mathcal{A}_s$ and the ground site s.

C. OVERALL METHODOLOGY

The overall Decomposed optimal Energy Management of UAV-based Cellular networks (D-EMUC) methodology consists of: i) solving the problem (8)-(10) to find the clusters $\mathcal{A}_s$ $\forall s \in \mathcal{S}$, ii) solving the problem (2)-(7),(11)-(14) for each $\mathcal{T}_i$ of each cluster $\mathcal{A}_s$.

VI. GENETIC ALGORITHM DESCRIPTION

Apart from targeting the solution of EMUC and D-EMUC, we design a new heuristic, called Genetic Algorithm for UAVs Planning on Large-Scale Scenarios (GAUP-LS). As suggested by its name, our solution aims at solving the problem in large-scale scenarios. To pursue this goal, we adopt a methodology based on a Genetic Algorithm (GA). We refer the reader to [46] for the main theory behind the branch of research of GAs, while here we report the main steps.

A. MOTIVATION

Although our problem may be solved by using different kind of metaheuristic algorithms, such as Single-State methods (e.g., Simulated Annealing, Tabu Search, etc.), or Population-based ones (e.g., GAs), Particle Swarm Optimization, Differential Evolution, etc.), we chose to use GAs since they have traditionally been used to tackle the routing problem in the networking context. More in depth, GA-based heuristics have been demonstrated to be well suited for proposing adaptive routing solutions on all-sized and all-type network scenarios. Starting from wireless environments, GAs have been exploited to solve routing-related problems in a variety of wireless settings, such as dynamic shortest path routing [47], [48], cluster-based schemes for MANETs [49], multicast [50] and broadcast routing [51]. If we move our attention to wired networking, the problem of dimensioning dynamic Wavelength Division Multiplexing (WDM) networks has been solved in [52] and [53] by exploiting the evolutionary concept of GAs. Moreover, several solutions based on GAs have also emerged to improve the energy efficiency of wireless [54], wired [55], and optical network scenarios [56].

B. CHROMOSOME AND FITNESS FUNCTION

Focusing on the set of chromosomes forming the population $\mathcal{M}$, each chromosome $c_M \in \mathcal{M}$ is denoted as a succession of $|\mathcal{D}| \times |\mathcal{T}|$ genes of type g_d^t representing the place $p \in \mathcal{P}$ where the UAV $d \in \mathcal{D}$ is located or moving to during

TS $t \in \mathcal{T}$. More formally, we define the chromosome as:

$$c_M = \left\{ g_1^1, ..., g_{|\mathcal{D}|}^1, ..., g_d^t, ..., g_1^{|\mathcal{T}|}, ..., g_{|\mathcal{D}|}^{|\mathcal{T}|} \right\} \quad (15)$$
$$\forall g_d^t \in [1, |\mathcal{P}|]; \forall d \in [1, |\mathcal{D}|]; \forall t \in [1, |\mathcal{T}|]$$

In our context, therefore, a chromosome represents a potential solution for the UAVs mission planning. In order to evaluate each solution and obtain the best one in terms of the pursued objective function, we define the following fitness function:

$$f(c_M) = \left(\sum_{s \in \mathcal{S}} \sum_{t \in \mathcal{T}} b_s^t + \alpha \cdot \sum_{g_d^t \in c_M} e_d^t \right) \psi \quad (16)$$

In the previous equation, the first term aggregates the sum of the battery level of each site b_s^t over the full set of TSs. The second term aggregates the energy level of each UAV d located at place g_d^t. Similarly to the objective function of EMUC, this term is multiplied by the weight α. However, differently from EMUC, we introduce a parameter, denoted as ψ, which is set to 1 if the solution represented by the current chromosome is feasible. Otherwise, if the current solution is not feasible, ψ is set to a low value (e.g., $\psi = \left(\left(B^{\text{MIN}} \cdot N_s^B \right) \cdot |\mathcal{S}| + E^{\text{MIN}} \cdot |\mathcal{D}| \right) \cdot |T|$), which is the least amount of total battery level on sites and on UAVs throughout the set of considered TSs. In order to assess the feasibility of the considered chromosome, a feasibility check function is applied to verify if the individual represents a solution that satisfies all the required constraints. The constraints that must be met are listed next:

1) **Coverage constraint.** Each area $a \in \mathcal{A} \subseteq \mathcal{P}$ must be covered at each TS $t \in \mathcal{T}$ by exactly one UAV $d \in \mathcal{D}$ (corresponding to constraint (3) of EMUC with $z_a^t = 0 \quad \forall a \in \mathcal{A}, t \in \mathcal{T}$);
2) **UAV battery level constraint.** The energy level of each UAV $d \in \mathcal{D}$ at each TS $t \in \mathcal{T}$ must be a value in the range $e_d^t = [E^{\text{MIN}}, E^{\text{MAX}}]$ (corresponding to constraint (7) of EMUC);
3) **Ground site battery level constraint.** The battery level of each site $s \in \mathcal{S} \subseteq \mathcal{P}$ at each TS $t \in \mathcal{T}$ must be a value in the range $b_s^t = [B^{\text{MIN}} \cdot N_s^{\text{B}}, B^{\text{MAX}} \cdot N_s^{\text{B}}]$ (corresponding to constraint of (5) of EMUC);
4) **Mission consistency constraint.** The action of each UAV $d \in \mathcal{D}$ at each TS $t > 0$ must be valid, i.e., a UAV is able to perform an action (e.g., STAY, REC, MOV, COV) only between admissible places. This condition corresponds to the existence of an arc $l \in \mathcal{L}$ with $t(l) = (g_d^{(t-1)}, t-1)$ and $h(l) = (g_d^t, t), \quad \forall t : t > 1 \in \mathcal{T}$ in the input graph of EMUC).

Finally, we stress the fact that both b_s^t and e_d^t depend on the procedure adopted to set the UAV actions, starting from the initial population, and detailed in the following subsection.

C. INITIAL POPULATION AND GENETIC OPERATORS

As regards the setup of the GAUP-LS algorithm, we generate suitable missions for the initial population by means of a keep covering strategy. The principles behind this strategy is to force the UAVs to consecutively cover the same area during the largest possible number of TSs. Clearly, a UAV $d_a \in \mathcal{D}$ has a maximum number of TSs, denoted with $\delta_{d_a}^{COV}$ in Eq. (17), during which it is able to consecutively perform coverage actions over the area $a \in \mathcal{A}$:

$$\delta_{d_a}^{\text{COV}} = \left\lfloor \frac{E^{MAX} - \max\{E_{a,s_i}^{\text{MOV}}\}}{E^{COV}} \right\rfloor; \forall s_i \in \mathcal{S} \quad (17)$$

where $\max\{E_{a,s_i}^{\text{MOV}}\}$ is the maximum amount of energy consumed by a UAV to reach the farthest site $s_i \in \mathcal{S}$ among the available ones in order to be recharged in the next TS. In addition, while a set of $|\mathcal{A}|$ UAVs covers the areas for $\delta_{d_a}^{\text{COV}}$ consecutive TSs, another fleet of UAVs staying on the sites will move to the closest areas in order to cover them during the next $\delta_{d_a}^{\text{COV}}$ TSs. Eventually, when a UAV ends its covering mission, it also moves to the closest site in order to be recharged. This process is iteratively repeated for the whole set of TSs.

In order to perform the evolution procedure, the genetic algorithms apply biologically inspired operators (selection, crossover, mutation) to the individuals in the population. In the GAUP-LS, these parameters were empirically set after performing different tests on the considered scenarios. Regarding the selection procedure, three different functions were tested: stochastic uniform, roulette wheel, and tournament selection. In order to crossover selected parents to create offspring that become part of the next generation, three different methods were analyzed: one-point, two-point, and uniform crossover. Finally, two additional mutation functions were tested to make small changes in the individuals of the population and create mutation children, namely Gaussian and uniform mutation. As a result of a set of experiments over the Frascati scenario, the 3-tuple of type $geneticOperators = \{selection, crossover, mutation\}$ that best fits the problem in terms of fitness function and computation time was $geneticOperators = \{roulette\_wheel, one-point, uniform\}$. From such previous results, this parameters setting is considered to be applied in our scenarios.

Therefore, the set of individuals which survive and form part of the next generation in the GAUP-LS algorithm is selected by applying the classical roulette wheel criterion. Moreover, the combination of individuals to generate offspring is performed by means of the single-point cross-over function. Regarding the mutation process, a two-step uniform mutation function is applied. First, a fraction of each individual is selected for mutation. Every gene in this fraction has a probability rate of being mutated. The second step is to replace each selected gene by another valid value. The application of selection, crossover and mutation operators is repeated in each generation of the GAUP-LS algorithm.

Once genetic operators are applied at each generation, a new population of chromosomes (i.e., the places visited by the UAVs) is formed. Thus, each new chromosome representing a potential set of UAV missions over $|\mathcal{T}|$ TSs must first

be checked in order to consider such solution as a valid one (ψ parameter in (16) of Sec. VI-B). The mission consistency constraint described in Sec. VI-B must be satisfied, as well as the ones related to coverage and maximum and minimum battery levels both on sites and on UAVs.

D. COMPLEXITY ANALYSIS

In the following, a complexity analysis of GAUP-LS is provided. Three variables must be considered for this analysis: i) population size $|\mathcal{M}|$, ii) chromosome length, denoted as $|c_M| = |\mathcal{D}| \cdot |\mathcal{T}|$, and iii) number of generations θ required by GAUP-LS to find the solution.

GAs complexity strongly depends on the fitness function to be optimized and on the type of genetic operators selected for crossover, offspring generation and genes mutation. In particular, the fitness function used by GAUP-LS during a particular generation, which is reported in eq. (16), takes $\mathcal{O}(|\mathcal{M}| \cdot |c_M|)$ to complete the evaluation of the whole population, $\mathcal{M}$. Since the choice of individuals to generate offspring follows the classical roulette wheel criterion, a complexity of $\mathcal{O}(|\mathcal{M}|)$ is associated for the selection procedure. Finally, the process of creating the new generation by means of crossover and mutation operators also requires $\mathcal{O}(|\mathcal{M}| \cdot |c_M|)$. Therefore, the GAUP-LS resulting complexity is $\mathcal{O}(|\mathcal{M}| \cdot |c_M| \cdot \theta)$.

VII. DESCRIPTION OF THE SCENARIOS

We define a set of realistic scenarios to assess the performance of EMUC, D-EMUC and GAUP-LS. We initially detail one scenario located in Frascati (Italy). In the following, we move our attention to a second scenario located in Cáceres (Spain).

A. FRASCATI SCENARIO

We initially consider a rural territory in Frascati, a town in the countryside of central Italy. Fig. 7(a) shows the aerial view of the considered zone. Interestingly, the terrain under consideration includes roads, fields, small houses, and buildings having at most 3-4 floors. Thanks to the fact that there are not tall obstacles (e.g., skyscrapers), this zone can be attractive for the deployment of a UAV-based cellular architecture. Fig. 7(b) reports the locations of the selected places, which are spread over the Frascati territory. In order to select the subset of installed sites over the set of places, we solve the minimum cost design problem of [57]. We refer the reader to [57] for the details. Fig. 7(c) reports the outcome in terms of installed sites. In addition, the centers of the areas to be covered and their boundaries (obtained through a simple Voronoi tessellation) are also reported. In this case, a set $\mathcal{S}$ of 3 sites and a set $\mathcal{A}$ of 8 areas are selected. Interestingly, a center of an area may be co-located with a ground site.

Tab. 2 summarizes the setting of the parameters in this scenario. More in depth, the solution of the problem of [57] allows also to dimension each site in terms of number of SPs and batteries, which are reported in the table. In addition, we have assumed a total number of UAVs much larger than the number of areas. In this way, we (possibly) ensure

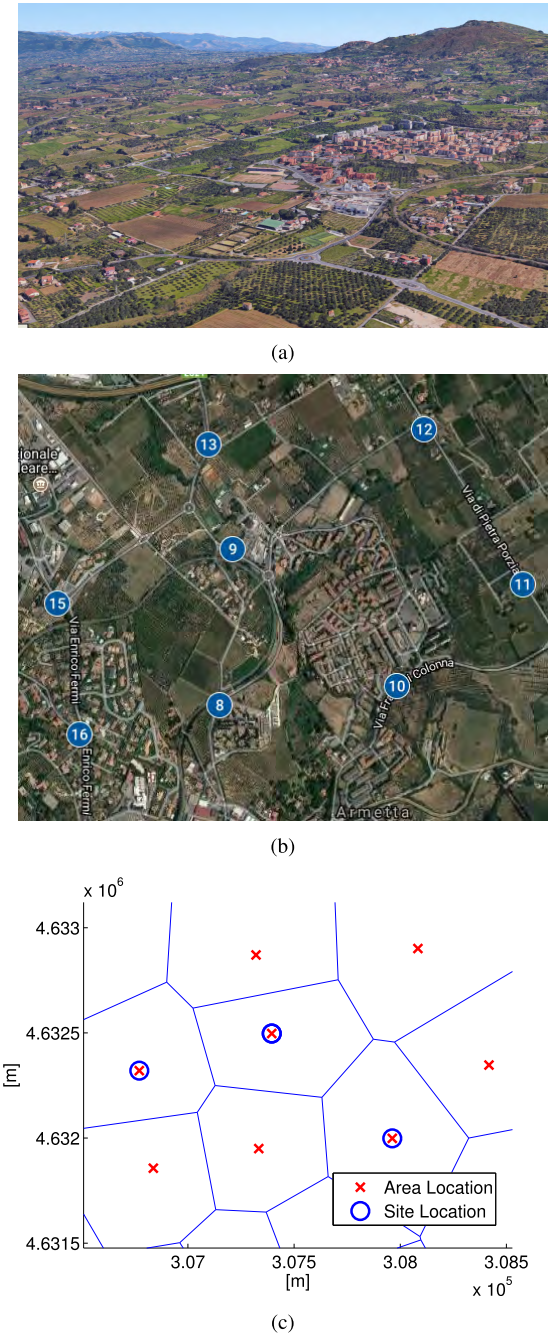

FIGURE 7. The Frascati scenario. (a) Aerial View (source: Google earth). (b) Locations of the places (source: Google earth). (c) Locations of the sites and the centers of the areas.

coverage over the territory in each TS, despite the fact that each UAV may be recharged, moved to an area, or moved to a site during a given TS.[2] Moreover, the minimum B^{MIN} and maximum B^{MAX} battery levels are set in accordance to [10]. We remark the fact that, while B^{MAX} is fundamental to satisfy the energy demand, the setting B^{MIN} is important to reduce as much as possible the detrimental effect of battery failure.

[2]The investigation of the impact of varying $|\mathcal{D}|$ is left for future work.

TABLE 2. Parameters setting for the Frascati scenario.

Parameter	Value
$\mathcal{A}$	$\{A8, A9, A10, A11, A12, A13, A15, A16\}$
$\lvert\mathcal{A}\rvert$	8
$\mathcal{S}$	$\{S9, S10, S15\}$
$\lvert\mathcal{S}\rvert$	3
$\mathcal{T}$	1 [day] divided in 24 TSs of 1 [h]
$\lvert\mathcal{D}\rvert$	25 UAVs
E^{COV}	200 [Wh]
E^{REC}	1000 [Wh]
E_s^t	see Fig.8
$E_{p1,p2}^{\text{MOV}}$	see Fig.9
N_s^{B}	$N_{S9}^{\text{B}} = 21$, $N_{S10}^{\text{B}} = 15$ $N_{S15}^{\text{B}} = 15$
N_s^{SP}	$N_{S9}^{\text{SP}} = 10$, $N_{S10}^{\text{SP}} = 8$, $N_{S15}^{\text{SP}} = 7$
B^{MIN}	720 [Wh]
B^{MAX}	2400 [Wh]
E^{MIN}	100 [Wh]
E^{MAX}	1000 [Wh]

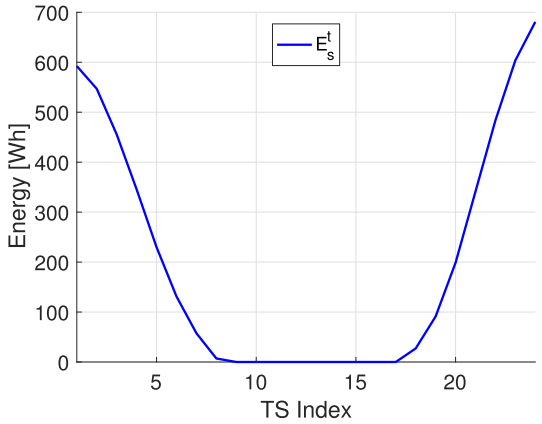

FIGURE 8. SP energy production (E_S^t [Wh]) - Frascati scenario.

In addition, the dimensioning of the number of SPs N_s^{SP} and the number of batteries N_s^{B}, whose values are reported in the table, is done by solving the dimensioning problem of [57]. In particular, the dimensioning aims at minimizing the total installation costs SPs and batteries, while taking into consideration the areas to be served and the energy produced by a single SP. Focusing on this last parameter, whose trend is shown in Fig. 8, we consider historical SP production data of Frascati from one day in June [58], which are obtained from the PVWatts calculator. In this way, we take into account realistic data, which are based on the weather conditions observed on the location for over 30 years. The resulting data are then the average energy production of the SP over the month under investigation. Clearly, the actual weather observed in the location may include also bad weather conditions that are different from the average trend. However, we point out that these variations may be easily introduced in the model of [57], and hence be reflected into a different set of batteries deployed in each site. Moreover, we point out that the SP energy production is also an input parameter of the problem studied in this work.

Focusing then on the parameters related to the energy consumption of the UAVs, we assume that each UAV can be

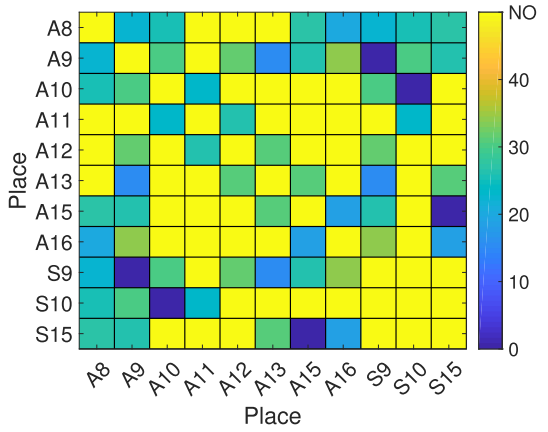

FIGURE 9. E_{p_1,p_2}^{MOV} $\forall p_1 \in \mathcal{P}, p_2 \in \mathcal{P}$ [Wh] (NOTE: Cells with value "NO" denote place pairs not connected with an $\mathcal{L}^{\text{MOV}}$ arc) - Frascati scenario.

charged up to $E^{\text{MAX}} = 1000$ [Wh]. Moreover, we assume that the UAV energy can be decreased up to a minimum value $E^{\text{MIN}} = 100$ [Wh]. In this way, each UAV has an amount of energy sufficiently high to safely land on a site upon an emergency and/or bad weather condition. In addition, Fig. 9 reports the energy values of the $\mathcal{L}^{\text{MOV}}$ arcs. Intuitively, we have set E_{p_1,p_2}^{MOV} $\forall p_1 \in P, p_2 \in \mathcal{P}$ by considering an amount of consumed energy proportional to the distance between p_1 and p_2. However, an arc is included only if the distance between p_1 and p_2 is lower than a maximum value, which is set equal to 900 [m]. In this way, for example, the distance between a site and the UAV serving an area can guarantee an adequate Signal To Interference plus Noise Ratio (SINR) for the backhaul radio link established between the site and the UAV.[3] Moreover, the value set for the maximum distance and the considered TS duration allow the UAV coming back to the ground site in one TS, which would be not always feasible (due to energy limitations and/or speed constraints) with larger distances and/or shorter TSs. Consequently, the $\mathcal{L}^{\text{MOV}}$ graph is not a full mesh (see the yellow cells of Fig. 9, corresponding to the "NO" label in the colorbar of the figure). In addition, there are places p_1 and p_2 with $E_{p_1,p_2}^{\text{MOV}} = 0$ [Wh], corresponding to: i) same areas or same sites pairs, or ii) area-site pairs which are co-located, and hence not consuming energy values for moving the UAVs between them (see e.g, the S10-A10 pair).

B. CÁCERES SCENARIO

In the following, we move our attention to the definition of a large-scale scenario located in Cáceres (Spain). The selected territory, spanning over an area 1,750 m^2, is reported in Fig. 1(a) (aerial view) and Fig. 10(b) (top view with place locations). Similarly to the Frascati scenario, we solve the minimum cost problem of [57] to retrieve the set of places, as well as the number of installed SPs and batteries. The resulting outcome is shown in Fig. 10(c) and in Tab. 3, while

[3] A more detailed evaluation of this aspect is left for future work.

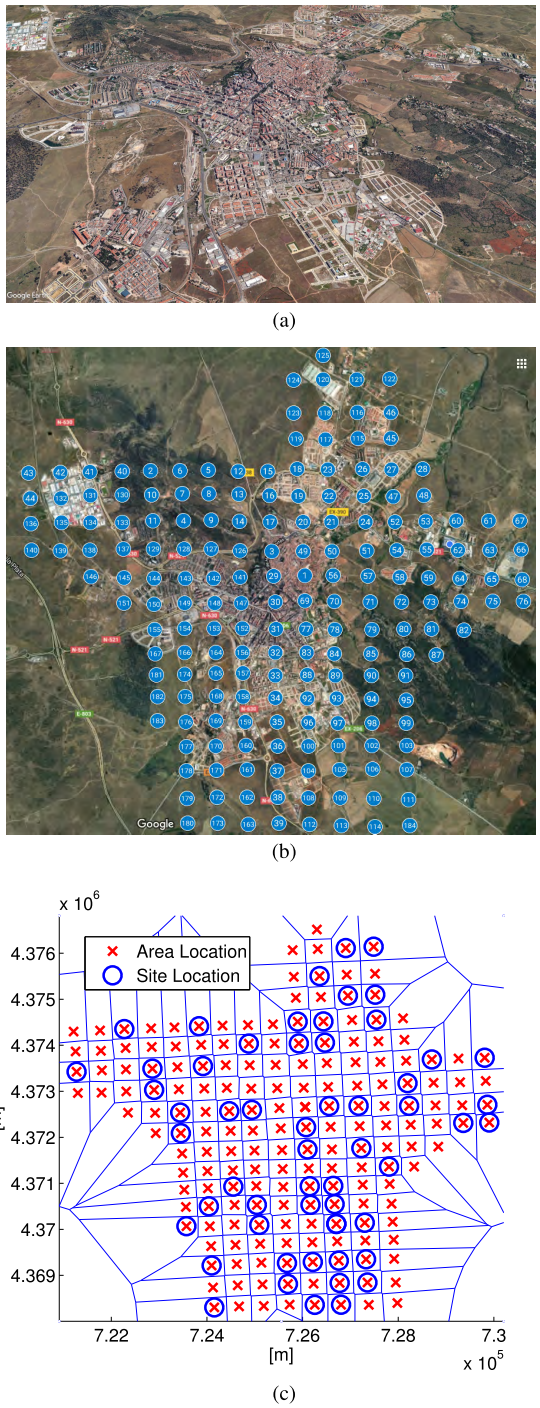

FIGURE 10. The Cáceres scenario. (a) Aerial view (source: Google earth). (b) Locations of the places (source: Google earth). (c) Locations of the sites and the centers of the areas.

Fig. 11 reports the SP energy during the month under consideration (i.e., June). As a result, we have $|\mathcal{A}| = 184$ areas and $|\mathcal{S}| = 56$ sites.

Focusing on the values of UAV energy needed to move between places ($E^{\text{MOV}}_{p_1,p_2}$), we adopt a similar procedure to the Frascati scenario. The resulting values of $E^{\text{MOV}}_{p_1,p_2}$ are reported in Fig. 12. Finally, we keep the same value as in the Frascati scenario for what concerns B^{MIN}, B^{MAX}, E^{MIN}, E^{MAX}.

TABLE 3. Parameters setting for the Cáceres scenario.

Parameter	Value
$\mathcal{A}$	$\{A1, \ldots, A184\}$
$\lvert\mathcal{A}\rvert$	184
$\mathcal{S}$	$\{S185, \ldots, S240\}$
$\lvert\mathcal{S}\rvert$	56
$\mathcal{T}$	1 [day] divided in 24 TSs of 1 [h]
$\mathcal{D}$	368 UAVs
E^{COV}	200 [Wh]
E^{REC}	1000 [Wh]
E^{t}_{s}	see Fig. 11
$E^{\text{MOV}}_{p1,p2}$	see Fig. 12
N^{IB}_{s}	16 (S23,S68,S76,S93,S105,S109,S113,S122), 19 (S45,S79,S97,S104,S106,S112,S115, S144,S158,S183), 22 (S4,S18,S37,S57,S60,S69,S88,S89,S92,S121,S178), 26 (S13,S19,S22,S27,S38,S55,S56,S67,S75,S77,S110,S118,S133, S137,S142,S175,S180), 29 (S6,S41,S59,S86,S98,S136,S141, S150,S159,S165)
N^{SP}_{s}	7 (S23,S68,S76,S93,S105,S109,S113,S122), 8 (S45,S79,S97,S104,S106,S112,S115, S144,S158,S183), 9 (S4,S18,S37,S57,S60,S69,S88,S89,S92,S121,S178), 10 (S13,S19,S22,S27,S38,S55,S56,S67,S75,S77,S110,S118,S133, S137,S142,S175,S180), 11 (S6,S41,S59,S86,S159), 13 (S98,S136,S141,S150,S165)
B^{MIN}	720 [Wh]
B^{MAX}	2400 [Wh]
E^{MIN}	100 [Wh]
E^{MAX}	1000 [Wh]

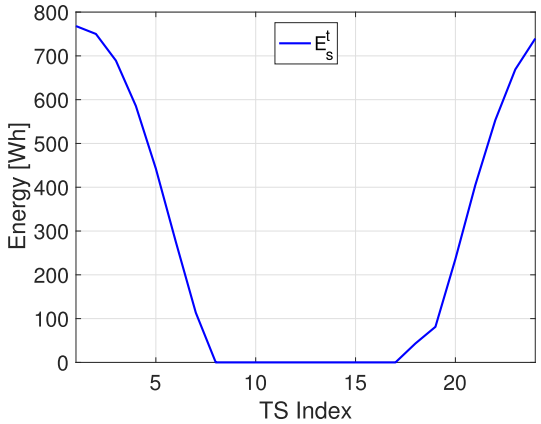

FIGURE 11. SP energy production (E^{t}_{s} [Wh] (Cáceres scenario).

VIII. RESULTS

We have implemented the EMU and D-EMUC in Cplex 12.7.1. Both the models are run on a high performance computing cluster, composed of four nodes, each of them with 32 cores and 64 GB of RAM. On the other hand, the GAUP-LS algorithm is coded in Matlab and run on a dual-core Intel-based machine at 3.1 GHz with 16 GB of RAM.

A. EVALUATION OF THE FRASCATI SCENARIO

We initially run EMUC, D-EMUC and GAUP-LS on the Frascati scenario. Focusing on the input parameters used to tune our algorithms, we assume a variation of $\alpha \in \{0.01, 0.1, 1, 10, 100\}$ to weigh differently the ground sites and the UAVs battery levels. In addition, we always set very large values of the penalty weight γ, in order to ensure that even a single area not covered during a single TS has an impact on the objective function. Specifically, we set $\gamma = 10^5$ when

TABLE 4. Breakdown of the results from the Frascati scenario.

Metric	Algorithm	$\alpha = 0.01$	$\alpha = 0.1$	$\alpha = 1$	$\alpha = 10$	$\alpha = 100$
Obj. Function [Wh]	EMUC	$2.77 \cdot 10^6$	$2.79 \cdot 10^6$	$3.02 \cdot 10^6$	$5.36 \cdot 10^6$	$31.99 \cdot 10^6$
	D-EMUC	$2.77 \cdot 10^6$	$2.80 \cdot 10^6$	$3.03 \cdot 10^6$	$5.39 \cdot 10^6$	$32.75 \cdot 10^6$
	GAUP-LS	$2.75 \cdot 10^6$	$2.79 \cdot 10^6$	$3.01 \cdot 10^6$	$5.36 \cdot 10^6$	$28.71 \cdot 10^6$
Sites Batt. Level [Wh]	Upper bound	$2.93 \cdot 10^6$				
	EMUC	$2.77 \cdot 10^6$	$2.77 \cdot 10^6$	$2.78 \cdot 10^6$	$2.71 \cdot 10^6$	$2.59 \cdot 10^6$
	D-EMUC	$2.77 \cdot 10^6$	$2.78 \cdot 10^6$	$2.77 \cdot 10^6$	$2.76 \cdot 10^6$	$2.65 \cdot 10^6$
	GAUP-LS	$2.75 \cdot 10^6$	$2.76 \cdot 10^6$	$2.76 \cdot 10^6$	$2.74 \cdot 10^6$	$2.71 \cdot 10^6$
	Lower bound	$0.88 \cdot 10^6$				
UAVs Batt. Level [Wh]	Upper bound	$6 \cdot 10^5$				
	EMUC	$2.41 \cdot 10^5$	$2.39 \cdot 10^5$	$2.43 \cdot 10^5$	$2.65 \cdot 10^5$	$2.94 \cdot 10^5$
	D-EMUC	$2.57 \cdot 10^5$	$2.58 \cdot 10^5$	$2.59 \cdot 10^5$	$2.63 \cdot 10^5$	$3.01 \cdot 10^5$
	GAUP-LS	$2.52 \cdot 10^5$	$2.56 \cdot 10^5$	$2.57 \cdot 10^5$	$2.62 \cdot 10^5$	$2.60 \cdot 10^5$
	Lower bound	$0.6 \cdot 10^5$				
Comp. Time [s]	EMUC	18000	18000	18000	18000	18000
	D-EMUC	10.16	10.75	10.10	6.79	19.11
	GAUP-LS	4.87	5.08	4.73	4.91	5.18
Not Covered TSs [%]	EMUC	0	0	0.52	0	10.41
	D-EMUC	0	0	0	0	12.05
	GAUP-LS	0	0	0	0	0

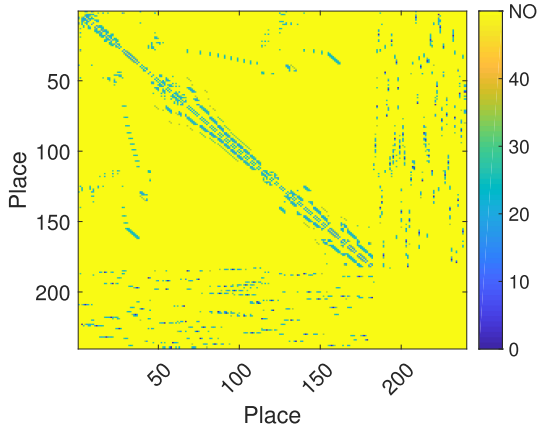

FIGURE 12. $E^{\text{MOV}}_{p_1,p_2}$ $\forall p_1 \in \mathcal{P}, p_2 \in \mathcal{P}$ [Wh] (NOTE: Cells with value "NO" denote place pairs not connected with an $\mathcal{L}^{\text{MOV}}$ arc) - Cáceres scenario (figure best viewed on screen).

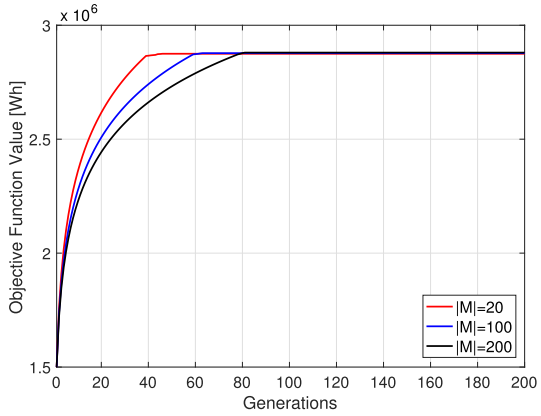

FIGURE 13. GAUP-LS convergence as a function of the population size, $|\mathcal{M}|$. - Frascati scenario.

$\alpha = \{0.01, 0.1, 1\}$ and $\gamma = 10^6$ when $\alpha = \{10, 100\}$. For what concerns the EMUC formulation, we set a maximum time limit of 18000 [s]. In case the computation is still running after this amount of time, we get the best solution retrieved so far. Focusing on the D-EMUC parameters, we assume a spatial decomposition over the three sites installed in this scenario. Moreover, a temporal decomposition of 6 sets of TS, each of them lasting for 4 hours, is assumed.

Since GAs are evolutionary metaheuristic algorithms, a (near) optimal solution is found after the execution of a set of iterations (generations). Generally, the quality of the solution is improved if the maximum number of generations to be set in the GA is increased. Another parameter to be tuned for improving such solution quality is the population size. However, if a big search space is considered, a penalty in the computation time must also be paid. Therefore, in order to set GAUP-LS parameters, we previously analyze the impact of varying the population size, $|M|$. Fig. 13 reports the convergence of GAUP-LS for different $|M|$ when $\alpha = 0.01$. Remarkably, when using the setting $|M| = 20$, GAUP-LS converges faster (around generation 40) than in the case where larger populations are considered. Moreover, as shown in Tab. 4, the computation time required to find the solution is reduced in comparison with EMUC and D-EMUC, while the optimality gap paid is negligible once the algorithm converges.

As a result of this analysis, we set a population size of $|M| = 20$ individuals, a maximum number of $\theta_{\text{MAX}} = 100 \cdot |c_M|$ generations, and a maximum number of $\tau = 50$ consecutive generations without improvement in the value of the fitness function (i.e., the average relative change in the best fitness function value over τ consecutive generations is less than or equal to a minimum value). Moreover, the type of mission defined for each UAV in the population follows the keep covering strategy described in Sec. VI.

Tab. 4 reports the breakdown of the results from the Frascati scenario, which are obtained by varying the α parameter. We report the total value of the objective function, as well as its main components, in terms of: i) total ground sites battery level $\sum_{s\in\mathcal{S}} \sum_{t\in\mathcal{T}} b^t_s$, ii) total UAVs battery level $\sum_{s\in\mathcal{S}} \sum_{t\in\mathcal{T}} e^t_s$. Focusing on the ground sites battery levels,

the table reports upper and lower bounds, which are computed as $\sum_{s\in\mathcal{S}} N_s^{\mathrm{B}} \cdot B^{\mathrm{MAX}}$ and $\sum_{s\in\mathcal{S}} N_s^{\mathrm{B}} \cdot B^{\mathrm{MIN}}$, respectively. Moreover, we report upper and lower bounds for the UAVs battery levels, which are computed as $|D| \cdot E^{\mathrm{MAX}}$ and $|D| \cdot E^{\mathrm{MIN}}$, respectively. In addition, the table includes the computation time (for D-EMUC it is defined as the summation of the computation time for all slots and all clusters considering a specific value of parameter α), as well as the percentage of the TSs during which an area is not covered by any UAV, which is computed as: $\sum_{p\in\mathcal{A}} \sum_{t\in\mathcal{T}} \frac{s_p^t}{|A|\cdot|T|}$.

Several considerations emerge from Tab. 4. First, the total values of the objective function tend to increase with α (as expected), due to the fact that this term multiples the UAVs battery level. Focusing then on the single terms of the objective function, we can see that, when α is increased, the battery level of the ground sites is reduced. This outcome suggests that, when the UAVs battery level becomes the predominant term, the best choice is to transfer the energy from the ground sites to the UAVs, in order to maximize their battery level. Clearly, the UAVs battery level tends to have a specular trend compared to the ground site battery level.

We then continue our analysis of Tab. 4 by comparing the outcomes of the different algorithms. Both D-EMUC and GAUP-LS perform very close to EMUC in terms of total objective function, ground sites battery level, and UAVs battery level for values of $\alpha < 100$. Interestingly, all the algorithms are pretty close to the upper bound of the total battery level of the ground sites. This is due the fact that our algorithms are able to efficiently exploit the SP energy to recharge the UAVs, while allowing an high amount of energy being stored in the battery of the site. Moreover, the UAVs battery level is clearly lower than the upper bound. This is due to the fact that the UAVs are used to cover portions of the territory, and hence during their missions they tend to deplete their batteries. Nevertheless, we can note that the UAVs battery level is strongly higher than the minimum one.

Focusing on the computation times of the different algorithms, both D-EMUC and GAUP-LS are able to retrieve a solution in few seconds at most, while EMUC strongly suffers from the complexity of the scenario, resulting in computation times of several hours. For this formulation, in fact, we have set a time limit of 5 [hours], and after this amount of time the best solution available so far has been retrieved. The percentage gap associated with the best obtained solution is about 5.5% for $\alpha \in \{0.01, 0.1, 1\}$ and it increases for higher values of α assuming respectively a value of 23.12% for $\alpha = 10$ and 36.73% for $\alpha = 100$. This poses challenges about the adoption of EMUC in a real deployment, where the management of the UAVs has to be performed in short time scales. On the contrary, both D-EMUC and GAUP-LS appear to be good candidates in this context. Observing the percentage of TSs in which an area is not covered by any UAV, we can note that this is equal to 0 with the exception of the solution provided by EMUC for $\alpha = 1$. However, we have to take into account that this solution is not an optimal one but just the best one found within the time limit, hence, it is a case in which the solution found leaves a not covered area in a certain TS.

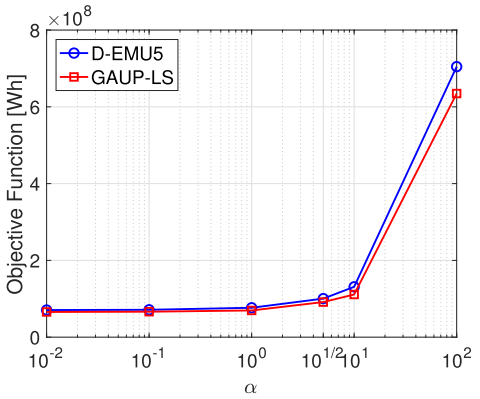

FIGURE 14. Objective function of D-EMUC and GAUP-LS vs. α - Cáceres scenario.

In the following, we concentrate our attention on the differences between the algorithms when $\alpha = 100$. Both EMUC and D-EMUC tend to perform better compared to GAUP-LS in terms of total objective function and UAVs battery level. By further investigating this issue, we have found that the percentage of not covered TSs is not negligible for EMUC and D-EMUC when $\alpha = 100$. In this case, in fact, keeping the UAVs fully recharged and not using them for territory coverage becomes an attractive choice, despite the relatively high penalty for not covering the areas. Moreover, we point out that GAUP-LS always ensure full coverage of the territory, resulting in a lower UAVs battery level compared to EMUC and D-EMUC.

B. EVALUATION OF THE CÁCERES SCENARIO

We then run our algorithms on the Cáceres scenario. In this case, the EMUC formulation is too challenging to be solved, mainly due to the large number of sites and areas (much larger than the Frascati scenario). Therefore, we concentrate our attention on D-EMUC and GAUP-LS, which are designed to tackle large problem instances. Similarly to the Frascati scenario, we consider a variation of $\alpha \in [0.01, 100]$. Moreover, we set the following parameters for D-EMUC: i) a penalty $\gamma = 10^5$ when $\alpha = \{0.01, 0.1, 1, 5\}$ and $\gamma = 10^6$ when $\alpha = \{10, 100\}$ (as in the Frascati scenario), ii) a spatial decomposition over the 56 ground sites characterizing this scenario and iii) a temporal decomposition of 6 sets of TS, each of them lasting for 4 hours. As in the case of the Frascati scenario, we set $|M| = 20$, $\theta_{\mathrm{MAX}} = 100 \cdot |c_M|$, and $\tau = 50$ for GAUP-LS, where the keep covering strategy is again used for UAVs missions in the initial population.

Fig. 14 reports the values of the objective function of D-EMUC and GAUP-LS. Also in this case, when α is increased, the total objective function tends to increase too. Compared to the Frascati scenario, the values of the objective function are almost two order of magnitude higher, due to the

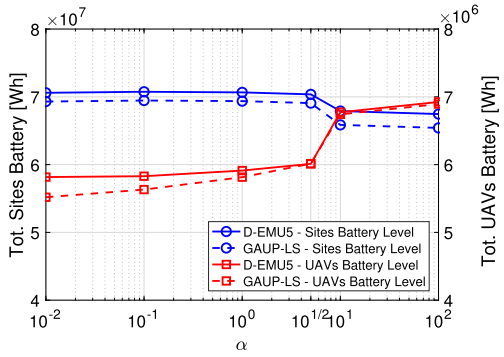

FIGURE 15. Battery levels of ground sites and UAVs vs. α - Cáceres scenario.

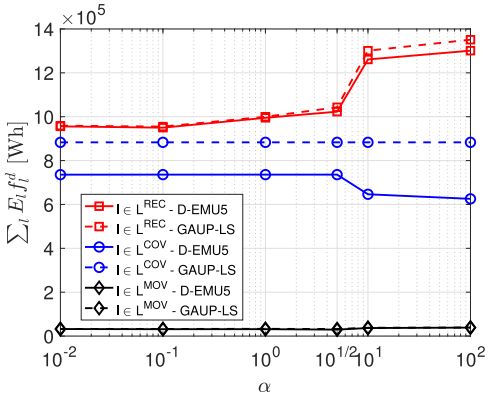

FIGURE 16. $\sum_l E_l f_l^d$ components for the different algorithms vs. α - Cáceres scenario.

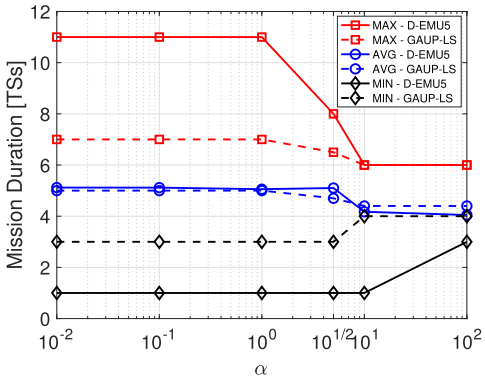

FIGURE 17. UAVs mission duration as a function of α.

increase in the number of sites as well as in the total number of UAVs.

In the following, we investigate the variation of the total battery levels for the ground sites and for the UAVs, as reported in Fig. 15. Interestingly, both the algorithms reveal a similar trend: when α is increased, the UAVs battery level tends to increase, while the ground sites battery level tends to decrease. However, we can note that D-EMUC tends to be more efficient than GAUP-LS, since the battery levels (for both UAVs and ground sites) are constantly higher for the former compared to the latter. This is due to the fact that D-EMUC applies a *divide et impera* approach, by splitting the original problem into smaller ones, and by optimally solving each subproblem. However, we stress the fact that GAUP-LS is always pretty close to D-EMUC.

In the next part, we shed light on the different components affecting the UAVs battery level e_d^t. We recall that e_d^t is computed from Eq. (6), by also ensuring that the resulting battery level is kept between minimum and maximum values through Eq. (7). By extending this metric to the whole set of TSs and UAVs, the different components of the total UAVs battery level are the following ones: i) total energy from COV actions $\sum_d \sum_{l \in \mathcal{L}^{\text{COV}}} E_l \cdot f_l^d$, ii) total energy for MOV actions $\sum_d \sum_{l \in \mathcal{L}^{\text{MOV}}} E_l \cdot f_l^d$ and iii) total energy for REC actions $\sum_d \sum_{l \in \mathcal{L}^{\text{REC}}} E_l \cdot f_l^d$. The three components are reported in Fig. 16 for D-EMUC and GAUP-LS vs. α. Interestingly, the largest amount of energy is due to UAVs recharging. However, the energy due to area coverage is also not negligible. Finally, the energy due to moving is lower compared to the previous two terms. This outcome suggests that, when the UAVs are used, they frequently cover the areas, while they tend to spend less energy in moving actions (possibly to the moving from a site to an area, and vice-versa). In addition, we can note that the total energy due to recharge tends to increase when α is increased. This results is expected, as maximizing the UAVs battery level is the predominant objective for large values of α. In addition, we can note that the energy due to coverage actions is decreased for D-EMUC when $\alpha \in \{10, 100\}$. By further investigating this issue, we have found that, in these cases, the percentage of not covered TSs is close to 10%, thus revealing that not all the areas are covered for the whole set of TSs. Finally, we also stress the fact that the term $\sum_d \sum_{l \in \mathcal{L}^{\text{REC}}} E_l \cdot f_l^d$ is a *potential* amount of energy injected to the UAVs. Thanks to Eq. (7), in fact, the UAV battery level e_d^t is saturated to E^{MAX}.

We then move our attention to the duration of the missions performed by the UAVs. More in depth, we define a mission as the number of TSs between two REC actions. Therefore, a mission can be a sequence of MOV, COV, REC and STAY actions. Fig. 17 reports the durations of the UAVs missions (in terms of TSs) for D-EMUC and GAUP-LS vs. α. The figure reports minimum, average, and maximum mission durations. Interestingly, we can note that the average mission duration is in the order of different TSs, thus suggesting that the UAV battery does not need to be recharged very frequently. However, the mission durations tends to decrease when $\alpha \in \{10, 100\}$. In this case, in fact, the problem tends to pursue the maximization of the UAV battery level, thus shortening the mission duration to guarantee high battery levels. Moreover, we can note that the minimum and maximum mission durations tend to the average one when $\alpha \in \{10, 100\}$, thus suggesting that the variability in the missions is also reduced, i.e., all UAVs tend to perform similar (short) missions. Finally, by comparing the GAUP-LS and D-EMUC trends, we can note that the average mission duration is pretty similar across the two algorithms. However, GAUP-LS

TABLE 5. Computation time of D-EMUC and GAUP-LS.

α	D-EMUC	GAUP-LS
0.01	2381.89 [s]	106.45 [s]
0.1	3645.63 [s]	113.38 [s]
1	5416.52 [s]	128.26 [s]
5	1464.92 [s]	115.91 [s]
10	2288.85 [s]	99.87 [s]
100	2121.85 [s]	96.90 [s]

enforces maximum and minimum mission duration closer to the average compared to D-EMUC.

In the last part of our work, we have compared D-EMUC and GAUP-LS in terms of computation time, as reported in Tab. 5. Interestingly, both the algorithms are able to retrieve a solution in a reasonable short amount of time. Moreover, we stress the fact that the D-EMUC time is computed by sequentially solving the different subproblems, and that this time may be further reduced by running in parallel the temporal decomposition for each site and each set of areas $\mathcal{A}_s$ retrieved during the spatial decomposition.

IX. DISCUSSION

We then discuss two main issues that may impact the presented results, namely: i) the introduction of wireless channel features, and ii) the consideration of battery ageing effects.

A. IMPACT OF WIRELESS CHANNEL CHARACTERISTICS

The features of the wireless channel are left outside the formulations and the algorithms. This is due to the fact that our primary goal is to study the impact on the battery levels of the ground sites and the UAVs as a consequence of the scheduling of the UAVs missions. Integrating the wireless channel characteristics, e.g., to ensure a minimum rate to users, would require to add the users in the formulations and the algorithms, thus dramatically complicating the considered problem. For example, Wu *et al.* [59] focus on the joint-aware trajectory and communication design in a UAV-based architecture. The considered model is a mixed-integer non-convex problem, which is solved in scenarios with at most two UAVs and one BS by means of an approximated technique. In addition, the impact on the UAV battery levels and the ground site battery level is not taken into account at all by [59]. Moreover, the scenarios considered in this work are 1-2 orders of magnitude larger than [59].

We also point out that our architecture is conceived to be applied in rural areas, where the connectivity is mainly provided by the UAVs. Hence, the primary goal is coverage, which is ensured when the UAV reaches the central location of an area. In this position, we assume that the channel characteristics are the best ones, i.e., short distance to users, Line-of-Sight conditions, and minimum interference with the neighboring UAVs.

Finally, focusing on bandwidth allocation, we assume that each UAV realizes a small cell. Therefore, a bandwidth of 5 [Mhz] can be assumed. Clearly, in case a single frequency is assumed for the UAVs, the set of areas, which is an input to our problem, should be built in such a way to limit the effect of interference among neighboring UAVs.

B. IMPACT OF BATTERY AGEING EFFECTS

In our work, we have assumed that the batteries of ground sites and of the UAVs are recharged and discharged over time. In the long-term, this operation may introduce ageing effects on the batteries, in terms e.g., of capacity degradation and lifetime. We then provide in the following some insights about this aspect, by drawing also some possible future research directions.

Focusing on the ground sites, we have assumed the exploitation of lead acid batteries. In this case, we always guarantee a minimum battery charge of 30% to ensure that the battery is kept in a healthy condition [10]. This setting should also prevent (up to a certain level), the ageing effects. Focusing instead on the UAVs, we have assumed lithium-based batteries. In this case, the ageing effects are strongly impacting the features of the battery. For example, Tröltzsch *et al.* in [60] reports a decrease in the battery capacity equal to 14% after some hundreds of cycles of discharge/charge. Moreover, the battery lifetime is limited to a maximum number of recharge/discharge cycles [61]. In our case, therefore, the capacity of the battery, and also its lifetime, may be influenced by the amount of REC actions performed by the UAVs. Both these features can be easily added to our model, as shown in the following.

Let us introduce the integer variables c_d^t, which store the number of REC actions for UAV d up to the current TS t. For a generic TS t, c_d^t is computed as:

$$c_d^t = c_d^{t-1} + \sum_{\substack{l \in \mathcal{L}^{\text{REC}}: \\ t(l)=(*,t-1) \\ h(l)=(*,t)}} f_l^d, \quad \forall d \in \mathcal{D}, t > 1 \in \mathcal{T} \tag{18}$$

Let us denote with C_d^{IN} the number of recharging actions that the UAV d has done in the past (from its first usage up to the initial TS of the current simulation). More formally, we have:

$$c_d^1 = C_d^{\text{IN}}, \quad \forall d \in \mathcal{D} \tag{19}$$

Let us denote now with $E^{\text{MAX}}(c_d^t)$ the maximum level of energy for UAV d at TS t after c_d^t transitions. The new energy bounds for the UAV are computed as:

$$E^{\text{MIN}} \leq e_d^t \leq E^{\text{MAX}}(c_d^t), \quad \forall d \in \mathcal{D}, t \in \mathcal{T} \tag{20}$$

Moreover, we need to include the binary variable y_d^t, which is equal to 0 when $c_d^{(t-1)}$ reaches a maximum number of transitions C_d^{MAX}, 1 otherwise. When this condition holds, the UAV d cannot be used any more, since it has reached its end of lifetime. More formally, we have:

$$y_d^t \leq (C^{\text{MAX}} - c_d^{(t-1)}), \quad \forall d \in \mathcal{D}, t \in \mathcal{T} \tag{21}$$

When y_d^t is 0, then all the MOV, REC and COV arcs are prevented for the current UAV (i.e., the UAV can be only in a

STAY state). More formally, we have:

$$f_l^d \leq y_d^t, \quad \forall l \in \mathcal{L}^{\text{MOV}} \cup \mathcal{L}^{\text{REC}} \cup \mathcal{L}^{\text{COV}} : t(l) = (*, t-1), h(l) = (*, t), d \in \mathcal{D}, t \in \mathcal{T} \quad (22)$$

Summarizing, we have introduced the ageing effect of capacity degradation in Eq. (20), the maximum number of REC actions in Eq. (21) and the auxiliary constraints of Eq. (18), Eq. (19), Eq. (22).

We then define the overall EMUC-AGE model by introducing in the EMUC one constraints (18)-(22). We then test EMUC-AGE over a simple, yet representative, example. More in detail, we consider the Frascati scenario with ageing parameters: $C_d^{\text{IN}} = 228 \quad \forall d \in \mathcal{D}$, $C_d^{\text{MAX}} = 230 \quad \forall d \in \mathcal{D}$, $E^{\text{MAX}}(c_d^t) = 986$ [Wh] (we assume a 14% of battery degradation in accordance to [60]). In this way, we test our problem in an extreme case, where all the UAVs have almost reached their end of lifetime. We then run the EMUC-AGE problem with $\alpha = 1$ and we retrieve a total objective function equal to $2.74 \cdot 10^6$ and 62.5% of not covered TSs. Both these metrics are clearly lower compared to the results obtained by EMUC in Tab. 4. This suggests that the ageing effects have an impact on the UAVs battery and consequently on the results. The evaluation of more detailed ageing models, including e.g., more complex interactions among the battery components and/or the physical properties, is an interesting aspect that is left for future work.

X. CONCLUSIONS AND FUTURE WORK

We have targeted the problem of jointly managing the battery levels of UAVs and ground sites in a cellular network powered by renewable energy sources. After formulating the EMUC problem, we have designed the D-EMUC and GAUP-LS algorithms to solve even large instances composed of dozens of sites and hundreds of areas. We have then built a set of representative case-studies, including a small scenario from Italy and a large one from Spain. Results demonstrate that both D-EMUC and GAUP-LS perform sufficiently close to EMUC, with a clear improvement in terms of computation times. In addition, we have investigated the trade-off between maximizing the UAVs battery level and maximizing the ground sites battery level, by showing also its impact in terms of coverage, energy components and UAVs mission duration.

We believe that this work is a first step towards a more comprehensive approach. To this aim, the control issues related to the communication aspects between the UAVs and the machine running the problem have to be faced as future work. In addition, another interesting topic is the modeling of the throughput provided to users, and how this term can be introduced in our problem. Eventually, the throughput constraints on the link of backhauling between the UAV and the ground site require a further study. Moreover, we will consider the impact of introducing different sources of energy, such as wind and geo-thermal ones. Further research will be also dedicated to study new different mathematical programming models and decomposition techniques or ad hoc optimal solution procedures (e.g., Branch&Bound). Finally, we plan to evaluate the impact of detailed ageing models for the batteries.

ACKNOWLEDGMENT

This paper was presented in part at the IEEE International Conference on Environmental Engineering (EE) [1], and in part at the 9th International Conference on Network of the Future (NoF 2018) [2].

REFERENCES

[1] L. Amorosi, L. Chiaraviglio, F. D'Andreagiovanni, and N. Blefari-Melazzi, "Energy-efficient mission planning of UAVs for 5G coverage in rural zones," in *Proc. IEEE Int. Conf. Environ. Eng. (EE)*, Mar. 2018, pp. 1–9.

[2] J. Galán-Jiménez, L. Chiaraviglio, L. Amorosi, and N. Blefari-Melazzi, "Multi-period mission planning of UAVs for 5G coverage in rural areas: A heuristic approach," in *Proc. 9th Int. Conf. Netw. Future*, Nov. 2018, pp. 52–59.

[3] O. Onireti, J. Qadir, M. A. Imran, and A. Sathiaseelan, "Will 5G see its blind side? Evolving 5g for universal internet access," in *Proc. workshop Global Access Internet All*, Aug. 2016, pp. 1–6.

[4] A. Karlsson, O. Al-Saadeh, A. Gusarov, R. V. R. Challa, S. Tombaz, and K. W. Sung, "Energy-efficient 5G deployment in rural areas," in *Proc. IEEE 12th Int. Conf. Wireless Mobile Comput., Netw. Commun.(WiMob)*, Oct. 2016, pp. 1–7.

[5] L. Chiaraviglio *et al.*, "5G in rural and low-income areas: Are we ready?" in *Proc. ITU Kaleidoscope ICTs Sustain. World*, Nov. 2016, pp. 1–8.

[6] M. Mozaffari, W. Saad, M. Bennis, and M. Debbah, "Drone small cells in the clouds: Design, deployment and performance analysis," in *Proc. IEEE Global Commun. Conf. (GLOBECOM)*, Dec. 2015, pp. 1–6.

[7] M. Mozaffari, A. T. Z. Kasgari, W. Saad, M. Bennis, and M. Debbah, "Beyond 5G with UAVs: Foundations of a 3D wireless cellular network," vol. 18, no. 1, pp. 357–372, Jan. 2019.

[8] L. Chiaraviglio *et al.*, "Bringing 5G into rural and low-income areas: Is it feasible?" *IEEE Commun. Standards Mag.*, vol. 1, no. 3, pp. 50–57, Sep. 2017.

[9] A. Trotta, M. Di Felice, F. Montori, K. R. Chowdhury, and L. Bononi, "Joint coverage, connectivity, and charging strategies for distributed UAV networks," *IEEE Trans. Robot.*, vol. 34, no. 4, pp. 883–900, Aug. 2018.

[10] Y. Zhang, M. Meo, R. Gerboni, and M. A. Marsan, "Minimum cost solar power systems for LTE macro base stations," *Comput. Netw.*, vol. 112, pp. 12–23, Jan. 2017.

[11] A. Otto, N. Agatz, J. Campbell, B. Golden, and E. Pesch, "Optimization approaches for civil applications of unmanned aerial vehicles (UAVs) or aerial drones: A survey," *Networks*, vol. 72, no. 4, pp. 411–458, 2018.

[12] S. Hayat, E. Yanmaz, and R. Muzaffar, "Survey on unmanned aerial vehicle networks for civil applications: A communications viewpoint," *IEEE Commun. Surveys Tuts.*, vol. 18, no. 4, pp. 2624–2661, 4th Quart., 2016.

[13] *Gartner Inc*. Accessed: Apr. 23, 2019. [Online]. Available: http://www.gartner.com/newsroom/id/3602317

[14] A. Trotta and F. D. , Andreagiovanni, M. D. Felice, E. Natalizio, and K. R. Chowdhury, "When UAVs ride a bus: Towards energy-efficient city-scale video surveillance," in *Proc. IEEE Conf. Comput. Commun.*, Apr. 2018, pp. 1043–1051.

[15] N. H. Motlagh, M. Bagaa, and T. Taleb, "UAV-based IoT platform: A crowd surveillance use case," *IEEE Commun. Mag.*, vol. 55, no. 2, pp. 128–134, Feb. 2017.

[16] R. Clarke, "The regulation of civilian drones' impacts on behavioural privacy," *Comput. Law Secur. Rev.*, vol. 30, no. 3, pp. 286–305, Jan. 2014.

[17] D. Gross. (2013). *Amazon Drone Delivery: How Would it Work?*. [Online]. Available: http://www.cnn.com/2013/12/02/tech/innovation/amazon-drones-questions/

[18] B. D. Song, K. Park, and J. Kim, "Persistent UAV delivery logistics: MILP formulation and efficient heuristic," *Comput. Ind. Eng.*, vol. 120, pp. 418–428, Jun. 2018.

[19] C. C. Murray and A. G. Chu, "The flying sidekick traveling salesman problem: Optimization of drone-assisted parcel delivery," *Transp. Res. C, Emerg. Technol.*, vol. 54, pp. 86–109, May 2015.

[20] S. Poikonen, X. Wang, and B. Golden, "The vehicle routing problem with drones: Extended models and connections," *Networks*, vol. 70, no. 1, pp. 34–43, Aug. 2017.

[21] I. Bor-Yaliniz and H. Yanikomeroglu, "The new frontier in RAN heterogeneity: Multi-tier drone-cells," *IEEE Commun. Mag.*, vol. 54, no. 11, pp. 48–55, Nov. 2016.
[22] M. Mozaffari, W. Saad, M. Bennis, and M. Debbah, "Unmanned aerial vehicle with underlaid device-to-device communications: Performance and tradeoffs," *IEEE Trans. Wireless Commun.*, vol. 15, no. 6, pp. 3949–3963, Jun. 2016.
[23] I. Bor-Yaliniz, M. Salem, G. Senerath, and H. Yanikomeroglu, "Is 5G ready for drones: A look into contemporary and prospective wireless networks from a standardization perspective," *IEEE Wireless Commun.*, vol. 26, no. 1, pp. 18–27, Feb. 2019.
[24] S. M. Adams and C. J. Friedland, "A survey of unmanned aerial vehicle (UAV) usage for imagery collection in disaster research and management," in *Proc. 9th Int. Workshop Remote Sens. Disaster Response*, 2011, p. 8.
[25] I. Maza, F. Caballero, J. Capitán, J. R. Martínez-de-Dios, and A. Ollero, "Experimental results in multi-UAV coordination for disaster management and civil security applications," *J. Intell. Robotic Syst.*, vol. 61, pp. 563–585, Jan. 2011.
[26] M. Asadpour, D. Giustiniano, K. A. Hummel, and S. Egli, "UAV networks in rescue missions," in *Proc. 8th ACM Int. Workshop Wireless Netw. Testbeds, Experim. Eval.*, New York, NY, USA: ACM, 2013, pp. 91–92.
[27] F. Malandrino, C. Chiasserini, C. Casetti, L. Chiaraviglio, and A. Senacheribbe. (2018). "Planning UAV activities for efficient user coverage in disaster areas." [Online]. Available: https://arxiv.org/abs/1811.12450
[28] M. Erdelj and N. Enrico, "UAV-assisted disaster management: Applications and open issues," in *Proc. Int. Conf. Comput., Netw. Commun. (ICNC)*, Feb. 2016, pp. 1–5.
[29] M. Erdelj, M. Król, and E. Natalizio, "Wireless sensor networks and multi-UAV systems for natural disaster management," *Comput. Netw.*, vol. 124, pp. 72–86, Sep. 2017.
[30] M. Erdelj, E. Natalizio, K. R. Chowdhury, and I. F. Akyildiz, "Help from the sky: Leveraging UAVs for disaster management," *IEEE Pervasive Comput.*, vol. 16, no. 1, pp. 24–32, Jan. 2017.
[31] M. Erdelj, B. Uk, D. Konam, and E. Natalizio, "From the eye of the storm: An IoT ecosystem made of sensors, smartphones and UAVS," *Sensors*, vol. 18, no. 11, p. 3814, 2018.
[32] M. Chen, M. Mozaffari, W. Saad, C. Yin, M. Debbah, and C. S. Hong, "Caching in the sky: Proactive deployment of cache-enabled unmanned aerial vehicles for optimized quality-of-experience," *IEEE J. Sel. Areas Commun.*, vol. 35, no. 5, pp. 1046–1061, May 2017.
[33] X. Cao, L. Liu, Y. Cheng, and X. S. Shen, "Towards energy-efficient wireless networking in the big data era: A survey," *IEEE Commun. Surveys Tuts.*, vol. 20, no. 1, pp. 303–332, 1st Quart., 2018.
[34] E. Yanmaz, S. Yahyanejad, B. Rinner, H. Hellwagner, and C. Bettstetter, "Drone networks: Communications, coordination, and sensing," *Ad Hoc Netw.*, vol. 68, pp. 1–15, Jan. 2018.
[35] J. Sánchez-García, J. García-Campos, M. Arzamendia, D. Reina, S. Toral, and D. Gregor, "A survey on unmanned aerial and aquatic vehicle multi-hop networks: Wireless communications, evaluation tools and applications," *Comput. Commun.*, vol. 119, pp. 43–65, Apr. 2018.
[36] D. G. Reina, H. Tawfik, and S. L. Toral, "Multi-subpopulation evolutionary algorithms for coverage deployment of UAV-networks," *Ad Hoc Netw.*, vol. 68, pp. 16–32, Jan. 2018.
[37] N. R. Zema, E. Natalizio, and E. Yanmaz, "An unmanned aerial vehicle network for sport event filming with communication constraints," in *Proc. BalkanCom 1st Int. Balkan Conf. Commun. Netw.*, May 2017, pp. 1–10.
[38] K. Dorling, J. Heinrichs, G. G. Messier, and S. Magierowski, "Vehicle routing problems for drone delivery," *IEEE Trans. Syst., Man, Cybern., Syst.*, vol. 47, no. 1, pp. 70–85, Jan. 2017.
[39] S. Karaman and E. Frazzoli, "Linear temporal logic vehicle routing with applications to multi-UAV mission planning," *Int. J. Robust Nonlinear Control*, vol. 21, no. 12, pp. 1372–1395, 2011.
[40] G. B. Lamont, J. N. Slear, and K. Melendez, "UAV swarm mission planning and routing using multi-objective evolutionary algorithms," in *Proc. IEEE Symp. Comput. Intell. Multi Criteria Decis. Making*, Apr. 2007, pp. 10–20.
[41] D. Kim and J. Lee, "Integrated topology management in flying ad hoc networks: Topology construction and adjustment," *IEEE Access*, vol. 6, pp. 61196–61211, 2018.
[42] R. Magán-Carríon, J. Camacho, P. García-Teodoro, E. F. Flushing, and G. A. D. Caro, "A dynamical relay node placement solution for manets," *Comput. Commun.*, vol. 114, pp. 36–50, Dec. 2017.
[43] L. Evers, T. Dollevoet, and A. I. Barros, "Robust UAV mission planning," *Ann. Oper. Res.*, vol. 222, pp. 293–315, Nov. 2014.
[44] J. Kim, B. D. Song, and J. R. Morrison, "On the scheduling of systems of UAVs and fuel service stations for long-term mission fulfillment," *J. Intell. Robotic Syst.*, vol. 70, nos. 1–4, pp. 347–359, Apr. 2013.
[45] F. D. Andreagiovanni, J. Krolikowski, and J. Pulaj, "A fast hybrid primal heuristic for multiband robust capacitated network design with multiple time periods," *Appl. Soft Comput.*, vol. 26, pp. 497–507, Jan. 2015.
[46] D. E. Goldberg and J. H. Holland, "Genetic algorithms and machine learning," *Mach. Learn.*, vol. 3, nos. 2–3, pp. 95–99, 1988.
[47] C. W. Ahn, S. Member, R. S. Ramakrishna, and S. Member, "A genetic algorithm for shortest path routing problem and the sizing of populations," *IEEE Trans. Evol. Comput.*, vol. 6 no. 6, pp. 566–579, Dec. 2002.
[48] S. Yang, H. Cheng, and F. Wang, "Genetic algorithms with immigrants and memory schemes for dynamic shortest path routing problems in mobile ad hoc networks," *IEEE Trans. Syst., Man, Cybern., C, Appl. Rev.*, vol. 40, no. 1, pp. 52–63, Jan. 2010.
[49] M. Al-Ghazal, A. El-Sayed, and H. Kelash, "Routing optimlzation using genetic algorithm in ad hoc networks," in *Proc. IEEE Int. Symp. Signal Process. Inf. Technol.*, Dec. 2007, pp. 497–503.
[50] N. Banerjee and S. K. Das, "Fast determination of QOS-based multicast routes in wireless networks using genetic algorithm," in *Proc. IEEE Int. Conf. Commun. Conf. Rec.*, vol. 8, Jun. 2001, pp. 2588–2592.
[51] S. Salcedo-Sanz, C. Bousono-Calzon, and A. R. Figueiras-Vidal, "A mixed neural-genetic algorithm for the broadcast scheduling problem," *IEEE Trans. Wireless Commun.*, vol. 2, no. 2, pp. 277–283, Mar. 2003.
[52] I. de Miguel, R. Vallejos, A. Beghelli, and R. J. Durán, "Genetic algorithm for joint routing and dimensioning of dynamic wdm networks," *IEEE/OSA J. Opt. Commun. Netw.*, vol. 1, no. 7, pp. 608–621, Dec. 2009.
[53] Z.-X. Wang, Z.-Q. Chen, and Z.-Z. Yuan, "QoS routing optimization strategy using genetic algorithm in optical fiber communication networks," *J. Comput. Sci. Technol.*, vol. 19, no. 2, pp. 213–217, Mar. 2004.
[54] Y. Wu and W. Liu, "Routing protocol based on genetic algorithm for energy harvesting-wireless sensor networks," *IET Wireless Sensor Syst.*, vol. 3, no. 2, pp. 112–118, Jun. 2013.
[55] J. Galán-Jiménez, "Legacy IP-upgraded SDN nodes tradeoff in energy-efficient hybrid IP/SDN networks," *Comput. Commun.*, vol. 114, pp. 106–123, Dec. 2017.
[56] J. Wang, X. Chen, C. Phillips, and Y. Yan, "Energy efficiency with QoS control in dynamic optical networks with SDN enabled integrated control plane," *Comput. Netw.*, vol. 78, pp. 57–67, Feb. 2015.
[57] L. Chiaraviglio, L. Amorosi, N. Blefari-Melazzi, P. Dell'Olmo, P. Monti, and C. Natalino, "Optimal design of 5G networks in rural zones with UAVS, optical rings, solar panels and batteries," in *Proc. 20th Int. Conf. Transparent Opt. Netw. (ICTON)*, Jul. 2018, pp. 1–4.
[58] B. Marion and M. Anderberg, "Pvwatts-an online performance calculator for grid-connected PV system," in *Proc. Solar Conf.*, 2000, pp. 119–124.
[59] Q. Wu, Y. Zeng, and R. Zhang, "Joint trajectory and communication design for multi-UAV enabled wireless networks," *IEEE Trans. Wireless Commun.*, vol. 17, no. 3, pp. 2109–2121, Mar. 2018.
[60] U. Tröltzsch, O. Kanoun, and H.-R. Tränkler, "Characterizing aging effects of lithium ion batteries by impedance spectroscopy," *Electrochimica Acta*, vol. 51, nos. 8–9, pp. 1664–1672, 2006.
[61] A. Warnecke. *Ageing Effects of Lithium-Ion Batteries*. Accessed: Apr. 23, 2019 [Online]. Available: http://www.batteries2020.eu/publications/201509EPE15/Ageing.pdf

LAVINIA AMOROSI received the Ph.D. degree in operational research from Sapienza University of Rome, in 2018. From 2017 to 2018, she was a Researcher with the Consorzio Nazionale Interuniversitario Delle Telecomunicazioni (CNIT) for the Superfluidity H2020 Project. She was a visiting Ph.D. student with the Lancaster University Management School, Lancaster, U.K., under the supervision of Prof. M. Ehrgott, in 2016; and also with the University of Seville, Spain, under the supervision of Prof. J. Puerto, in 2017. She is currently holding a postdoctoral position with the Department of Statistical Sciences, Sapienza University of Rome. Her research areas are combinatorial optimization, with the particular interest in network optimization and multiobjective programming.

LUCA CHIARAVIGLIO (M'09–SM'16) received the Ph.D. degree in telecommunication and electronics engineering from the Politecnico di Torino, Italy. During the past years, he has spent research periods with Boston University, Boston, MA, USA; INRIA Sophia Antipolis, France; Auckland University of Technology, New Zealand; and ETECSA S.A., Cuba. He is currently a Tenure Track Assistant Professor with the Networking Group, Department of Electronic Engineering, University of Rome Tor Vergata, Italy. He has coauthored over 120 papers published in international journals and conferences, and has collaborated with more than 150 coauthors, which are affiliated with over 40 national and international institutions. He participates in the TPC of top-leading conferences, including the IEEE INFOCOM, the IEEE GLOBECOM, the IEEE ICC, the IEEE VTC, and the IEEE GlobalSIP. According to Google Scholar, his H-Index is 29. His current research interests include 5G networks, cloud computing, optimization applied to telecommunication networks, electromagnetic fields, and new architectures to reduce the digital divide in rural and low-income areas. He is a member of the organizing committee of several conferences, such as ECOC, LANMAN, and 5G-Italy. He is a Founding Member of the IEEE Communications Society Technical Subcommittee on Green Communications and Computing. He is currently the Coordinator of the national project BRIGHT: Bringing 5G Connectivity in Rural and Low-Income Areas. During the last years, he has been involved in different European projects, such as the H2020 5G-EVE, H2020 Superfluidity, FP7 Trend, FP7 EcoNet, and FP7 Bone. He has received the Best Paper Award in different conferences, including the IEEE VTC and the ICIN. Some of his papers are listed as Best Readings on Green Communications by the IEEE. Moreover, he has been recognized as an author in the top 1% most highly cited papers in the ICT field worldwide. His papers "Optimal Energy Savings in Cellular Access Networks" and "Reducing Power Consumption in Backbone Networks" are the most cited papers from all the IEEE ICC conferences and the IEEE ICC workshops in the period 2009–2018 (Source: Scopus). He is in the Editorial Board of the *IEEE Communications Magazine*, the IEEE ACCESS, and the IEEE TRANSACTIONS ON GREEN COMMUNICATIONS AND NETWORKING.

JAIME GALÁN-JIMÉNEZ received the Ph.D. degree in computer science and communications from the University of Extremadura, Spain, in 2014. He is currently with the Computer Science and Communications Engineering Department, University of Extremadura, as an Assistant Professor. In 2018, he received the Teaching Excellence Award from the University of Extremadura. During the past years, he has spent several research and teaching periods with the University of Rome Tor Vergata, and also with the University of Rome La Sapienza, Italy. His main research interests are 5G networks planning and design, 5G provisioning in rural and low-income areas, software-defined networks, traffic matrix estimation, and mobile ad-hoc networks.